What's the Diel with this Signal?

Jason Albright
Nathaniel Gustafson
Michaeline Nelson
Bianca Rodriguez-Cardona
Chris Shughrue

Abstract:

Evapotranspiration(ET) induced diel fluctuations in stream discharge highlight relationships between hydrological and ecological processes. Diel fluctuations have been well observed at the HJ Andrews Experimental Forest in the Western Cascades for several decades and recent advancements is sensor technology have made it ever easier to quantify these small changes and monitor them over shorter time scales to create higher resolution data. In this study we compiled pre-existing stream discharge and air temperature data collected at the Andrews over the previous 10 years to examine phase lags between minimum stream discharge and maximum air temperature. We conducted several field studies to compare lithological characteristics of two specific watersheds and installed capacitance rods in higher reaches in order to analyze the presence and timing of signals in stream height to compare to those present at the downstream v-notch weirs. Field surveys and data from the capacitance rods in both watersheds revealed that diel signals were most strongly exhibited in vegetated alluvial reaches and signals in bedrock reaches were significantly weaker. To investigate these disparities we utilized LiDAR data to extract tree heights to estimate the total transpiration from riparian vegetation. These findings show that estimated ET from only riparian vegetation can account for the ET loss from the total discharge. In order to further the conceptual understanding of ET from riparian vegetation and its strong interaction with overland flow in streams we built a simple mathematical model describing the outflow from stream banks as a function of ET.

Introduction:

Historical Note: At the onset of the work, we inverted several rulers at various locations in streams to gauge stream height fluctuations throughout a 24-hr period. Any graduated pillar used in this fashion is variously referred to as a nilometer, and as it turns out the history behind this name is quite intriguing. Ancient Egyptians, farming in the floodwaters of Nile, monitored and recorded annual flood levels at the beginning of each season in order to estimate the yield of their crops. Today, three thousand years later, stream levels continue to be monitored using a variety of more sophisticated tools whose function does not differ from that of the original nilometers implemented by the Egyptians.

River basin stream flow and ground water levels exhibit two distinct trends after the cessation of precipitation, during the subsequent period of sustained run off. The first is a seasonal trend characterized by the persistence of diminishing stream flow rates and water table levels as water stored in the soil is released. The second is a daily pattern of fluctuating stream flow variously linked to variety of mechanisms including freeze-thaw patterns, precipitation, anthropogenic activities and evapotranspiration(ET). Historically much literature has been published regarding the long-term changes, while shorter cycles have not been as extensively studied (Gribovszki et al. 2010). Recently, the development of high frequency digital data collection devices has allowed for increased study of the diel (24h) cycles that can be difficult to detect visually and even more difficult to quantify from these measurements. Information from the study of these diel cycles has the potential to be used in observing

coupling between the hydrological and biological cycle in watersheds as well as for water resource management purposes (Barnard et al. 2010, Bond et al. 2002, Gribovszki et al. 2010).

Diel fluctuations measured by changes in stream discharge during periods of little rain and low stream flow induced primarily by ET have been observed and studied by researchers since the 1930's when Blaney et al. detected a diel signal in stage height in the Santa Ana River in California (Blaney et al. 1930 and 1933, Gribovszki et al 2010). Since this time these signals have been documented in studies in a variety of locations in the US including North Carlolina(Dunford and Fletcher, 1947) and Utah(White, 1932), and also in Hungary(Gribovszki, 2008), Austria(Bousek, 1933), and South Africa(Wicht, 1942) and several others in the literature.T These changes in flow have been attributed to solar radiation and air temperature and linked to the diurnal cycle of riparian ET (Bond et al. 2002, Moore et al. 2004, Wondzell et al. 2006, Gribovszki 2008). Diel signals, first recorded in the groundwater-levels and later recorded in stream flow, have been used to estimate ET over an area (Gribovszki et al. 2010).

Diel fluctuations have been closely monitored and recorded over the past decade at the HJ Andrews Experimental Forest in the western Cascades of Oregon, USA. Previous work related to diel signals conducted in these watersheds include studies by Bond et al. 2002, Wondzell et al. 2006, Wondzell et al. 2007, Wondzell et al. 2010 and Barnard et al. 2010. This previous research focused on the influence of vegetation on the diel patterns in stream flow and water table levels, the effect of morphology and discharge on hyporheic exchange flow, the influence of stream flow velocity on the diel signal, and the influence of transpiration on subsurface flow. In addition several of these studies attempt to create conceptual and mechanistic models describing hyporheic exchange patterns and diel signals. In our research we examined the following questions: 1) How are ET induced signals affected by base-flow levels and watershed characteristics? 2) Are diel signals synchronized across the watershed? 3) Does channel morphology influence diel signals? 4) What are the mechanisms for the influence of ET on diel fluctuations? 5) Assuming the diel signal is local and additive over channel length, does sap flow in vegetated alluvial channel account for observed diel fluctuations at the stream gauge?

Study Site Description

Our field study was conducted in Watershed 1(WS1) and Watershed 2(WS2) within the H.J. Andrews Forest (HJA) in the western cascades of Oregon, USA (Fig 1). The Andrews has a temperate marine climate, with wet winters and dry summers and 80% of rain falling between October and April. WS1 is 95.9 hectares with a minimum elevation of 457m and a maximum of 1027m, a 59% slope and a channel length of 2808m. Watershed 1 was clear-cut in the 1960's, now Red Alder (*Alnus rubra*) dominates the stream channel while young Douglass firs (*Pseudotsuga menziesii*) dominate the slopes. Stream channels are mostly alluvial deposits with debris causing steps and pools and short stretches of rapid flow over bedrock. A series of wells that extend across the stream and up the hillslope were placed in the WS1 lower channel just above the stream gauge (Fig. 2). WS2 is 60.3 hectares with a minimum elevation of 548m and a maximum of 1078m, a 53% slope and a channel length of 1861m. WS2 is an old growth forest with a Western Hemlock (*Tsuga heterophylla*) understory and an overstory of Douglas-fir (*Pseudotsuga menziesii)*. The stream channel splits into two separate channels (distance from) the stream gauge. The left channel is mostly exposed bedrock with shallow hill slopes and few trees growing in close proximity to the stream. The right channel is mostly alluvial with steeper banks and trees growing in and along the channel. (average discharge for both WS during summer) Both watersheds show high non-localized infiltration rates with percolation rates greater than 12cm/hr due to

the large presence and size distribution of pore spaces (Sheperd, 2006). In addition we analyzed data from additional watersheds in the HJA including WS3, WS6, WS7, WS8, WS9, WS10 (Table 1)

1) How are ET induced signals affected by base-flow levels and watershed characteristics?

Objective

Previous work by Bond et al. 2002 studying diel fluctuations in the HJA watersheds using data from the summer of 2000 examined the phase shift, the time lag between maximum transpiration and minimum stream discharge, and the correlation strength at that time lag. Our research extends this study by analyzing data from multiple years and across multiple watersheds at HJA in order to gain a better understanding of the influence behind the diel signal and the timing of the signal.

Methods

To examine phase shift (time lag) between maximum transpiration and minimum stream discharge, we graphed cross correlations between air temperature and stream discharge in R using Pearson's correlation coefficient (r). These graphs show the correlation (Y axis) as a function of lag time (X axis). Using data from WS1, WS2, WS3, WS6, WS7, WS8, WS9, WS10 from 2005 to 2009, we plotted correlations for 5 successive weeks (June 26th to August 1st). These weeks in most years correspond to summer baseflow when the diel signal is strongest, in an interval spanning form wet to increasingly dry conditions. Additionally we wanted to see if lag times varied in years of high versus low precipitation. In WS1 we examined 10 years of data from 2000 through 2009 during the week of July 1st to July 7th. We chose this week because diel signals were observed during this time in all years. We compared these graphs to stream discharge and precipitation graphs for these ten years.

Results

Hydrographs from all the watersheds examined show diel fluctuation signals, however cross-correlation values of this discharge and air temperature were consistently low in WS2, WS3, WS6, WS7, and WS8. In these watersheds the minima on the graphed curves, corresponding to the number of hours from maximum air temperature to minimum discharge, ranged between r = - 0.4 to r = 0.1. In WS1, WS9, WS10 the air temperature and discharge signals are much more correlated with most r values occurring between .7 and .9, with various outliers.

The highest magnitude diel signals in the HJA watersheds occur in WS1. During some years when discharge levels are lower and there is a lack of precipitation in the late spring diel fluctuations can be observed beginning early in the season around mid-May and persisting until mid-July. This is apparent in WS1 in the years of 2002, 2003, and 2007. In years 2000, 2004, 2005, and 2008 higher precipitation persisted in the area until mid June (Fig. 3, Fig. 4). In these years discharge from the streams was much higher. Once precipitation terminated diel fluctuations could be better observed and continued into late August. At this time precipitation increases lead to disturbances in the signal, however, the signal is still noticeable in dry weeks following precipitation events in the beginning of the

fall. In each case the most obvious fluctuations lasted around 2 months before the signal became too weak due to drought, or were disturbed by precipitation events. In WS1 it is apparent that the amount of discharge is correlated with the phase lag of the diel signal. This can be seen in two ways 1) Looking at 5 weeks in a single summer, the time lag increases from around 4 hours to around 9 hours (Fig. 5) and 2) Looking at the time lag from July 1 to July 7 for 10 years, the time lags were least in years with the highest stream discharge (Fig. 6). This data supports a hill slope transpiration study measuring pre and post irrigation time lags on watershed hill slopes. Barnard et al. 2010 found that time lags between transpiration and hill slope discharge decreased in the post-irrigation period (Barnard et al. 2010).

The other two watersheds with high correlations between air temperature and stream discharge were WS9 and WS10. WS10 differed from WS1 because although it had high correlations time lags changed little over the 5 weeks and over 5 years. In WS10 discharge minimum lagged peak temperatures between 3 and 5 hours and did not show a clear trend from the beginning to end of the summer (Fig 7). WS9 was similar to WS10 except that discharge minima lagged peak temperatures slightly more, between 4 and 6 hours and correlations were generally stronger in the last few weeks (Fig 8).

Examining phase shifts plots over a time span of ten years and across various watersheds in HJA raised a couple of questions: 1) Why do WS1, WS9, and WS10 show signals that correlate with air temperature, while WS2, WS3, WS6, WS7 and WS8 signals don't correlate? 2) Why does WS1 behave differently from WS9 and WS10?

2) Are diel fluctuations synchronized across a watershed?

3) Does channel morphology influence diel fluctuations?

Objectives

Diel fluctuations have been measured by changes in stage height and discharge at stream gauges at the base of the stream, however the extent of these fluctuations over a larger stream network has not been examined. Our first goal was to see if we could observe diel fluctuations in various lower order streams above the gauging stations. In addition we wanted to observe how the phases of the peaks and troughs of these signals compared in order to test the 'connectivity' of the whole watershed stream system. Secondly, in hiking up WS2 one of our first observations was the difference in stream channel vegetation in bedrock versus alluvium channels. By setting up staff gauges in both streams in locations with similar channel width, water depth, and outflow, we wanted to see if the magnitude of stage height changes differed depending on the morphology of the channel.

Methods

To record changes in stage height along the stream, we set up staff gauges (rulers) along WS1 and WS2 (map). We conducted two 24-hour surveys in WS2 (July 7- July 8 and July 14- July15) and and a 48-hour survey (July 13- July 15) inWS1, taking measurements of stage height and water temperature every two to three hours. In WS1 we set up a total of 6 rulers and in WS2 7 rulers. Additionally, in WS1 we performed a 48-hour survey (July 12 - July 13) in the well networks D through G, with a total of 24 wells, measuring well depth every two to three hours. A survey was conducted of the surrounding well area to create a map of the area. We accounted for trees by measuring their circumference and in addition accounted for rocks, logs, and pools in reference to the wells (Fig 2).

After conducting these initial experiments, we obtained 4 WT-HR Trutrack capacitance rods, which we set up in the watersheds to collect more precise data. The capacitance rods record measurements every 15 minutes. We placed the 4 capacitance rods in WS2 from July 28th to August 5th and then moved these rods WS1 for August 5th to August 11th. By distributing the capacitance rods over a larger stream network we wanted to compare stage height changes over a larger area of the watershed and examine phases. We hiked along the reaches of large portions of WS1 and WS2. Superficial observations where made regarding alluvial or bedrock reaches, log jams, debris in channel and inferred exchange between surface and subsurface flow.

Results

a. Presence and Timing of the Diel Signal over a Larger Stream Network

From our staff gauge data, we observed that diel signals could be measured over a larger stream network within WS1 and WS2. Previously, diel signals in the HJ Andrews' watersheds have been measured in each watershed from a single V-notch weir located near the base of the stream. In WS1 our 48-hour ruler survey demonstrated that the diel signals are in phase in disparate points in the watershed. The signals are present in stream branches of various sizes that contribute to the main stream flowing down to the weir (Fig. 8). Two capacitance rods set up in WS1 collected data from August 5th to 12th. A diel signal was visible in this data and again supported that the diel signal is in phase throughout the watershed (Fig. 9). The 48-hour well survey in WS1 also showed diel signals demonstrating that the ground water is behaving in a similar manner as the stream.

b. Diel Signal Observations related to Channel Morphology

In WS2 our main objective was to see if bedrock and alluvium channels behaved differently. Our initial staff gauge observations consistently showed much larger changes in stage height in the alluvium channels than the bedrock channels. The capacitance rods set in WS2 to measure stage height further confirm this data. In WS2 the staff gauges that was set up in the channel with few to no trees or vegetation in the stream with bedrock reaches showed very little change in stage height. On the other hand, the rod set up in the channel with more alluvium and vegetation growing within the channel showed significant variation even though stream flow was lower (Fig. 9). Stage height is not a completely accurate measure of signals because it does not take into account the area of water flow. For this reason, the data at the stream gauges is calculated using V-notch weirs, which funnel all the water through one area and use the weir angle measurement to get more accurate discharge measurements. However, our staff gauge experiments demonstrated that variances in the flow related to the diel signal can be observed on a qualitative level using raw stage height data. Therefore, the small changes in stage height of the bedrock channel compared to the large changes in the alluvium channel suggest that the in stream vegetation plays a role in the diel stream signal. In addition our two capacitance rods in WS2 were set up in channels with similar sizes and water depths. Our surveys of WS1 did not show any significant differences in channel morphology.

4) What are the mechanisms for the influence of ET on diel fluctuations?

A Mathematical Treatment of Ground Water Outflow

Objectives

The main aim of this research was to build a simple mathematical model of outflow from a riparian aquifer in order to describe a potential mechanism behind the evapotranspiration(ET) induced diel fluctuation is stream height, and to also explore to effect of ET on the on the water table.

We begin with a analogy to outline the thought process behind this investigation. Consider a steadily pumped well located near a small river. If enough water were pumped from the well, then the water table would be drawn down. If this process were continued, then eventually the discharge of the river would decrease as a result of water feeding the well. The water loss from the river into the well is a result the change in shape of the water table. This change is depicted in the diagram below:

Diagram 1:

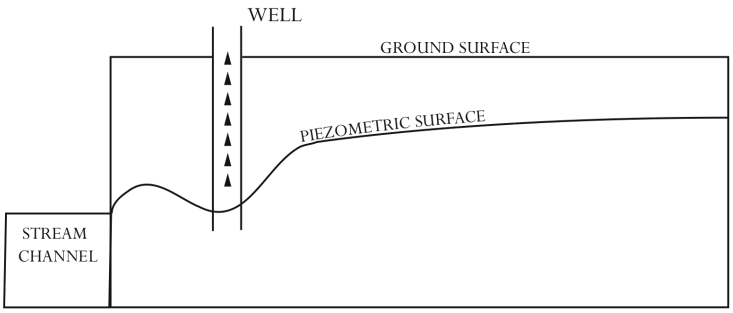

Model Description:

If we think of trees and other rooted vegetation growing along the banks of rivers and streams as a network of pumps driven by solar radiation, then when the sun is up some volume of water traveling along the main stream channel is trapped by tree roots. Our question becomes: can riparian vegetation draw enough water from the main stream channel to induce the observed fluctuations in stream discharge? To that end, consider an unconfined riparian aquifer as depicted in the schematic drawing below.

Diagram 2 :

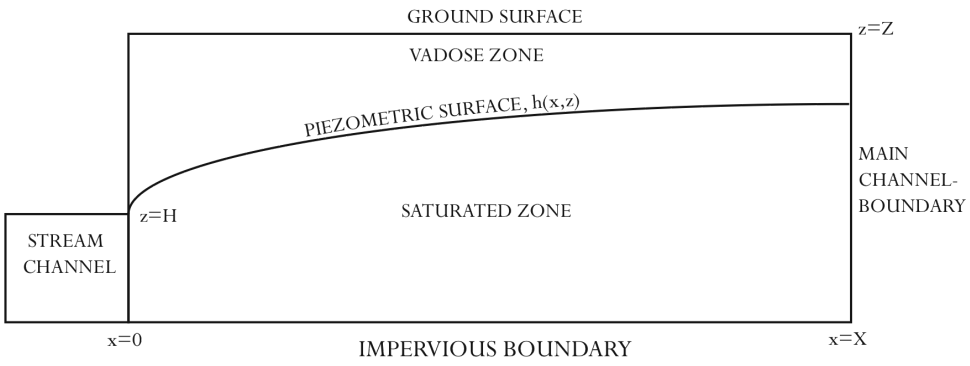

This schematic drawing represents an idealized version of an aquifer system, sufficiently simplified to bear mathematical treatment. Accordingly, we assume the rate of flow in the y-direction, oriented along the axis pointing out of the page, is insignificant in comparison to flow in the x and z-directions. It is also useful to break down all underground flow into either saturated flow or unsaturated flow. The upper boundary of the water table is often called a piezometric surface. Pore spaces in the soil are assumed to be completely filled with water below the piezometric surface, ergo this region is called the saturated zone. Above the water table lies the vadose zone, which categorizes the volume of water above the piezometric surface. Unsaturated flow occurs in the vadose zone where pores are only partially filled with water. In this model we only consider flow in the saturated zone.

Suppose further that the soil throughout the ideal aquifer is homogeneous and isotropic. Homogeneous means that if a small soil sample were cut out, the properties of the sample would be representative of the entire aquifer. In particular, the assumption that the sample is isotropic implies that the hydraulic conductivity of the soil in the horizontal direction and the vertical direction are equivalent. Under these assumptions, flow through the saturated zone is modeled using Darcy's law and the Poisson equation[3].

Darcy's Law

$$q = -k \cdot \left(\frac{\partial h}{\partial x} + \frac{\partial h}{\partial z}\right) \tag{1}$$

Darcy's law says that the volumetric rate of flow per unit cross sectional area, or specific volumetric flux, q, is proportional to the gradient of piezometric head, h. The constant of proportionality, k is called the hydraulic conductivity and it is a function of the permeability and porosity of the soil, which quantify the particular packing and distribution of pore size of the soil, respectively.

In order to understand the concept of hydraulic head consider the following example. If a well were dug into an aquifer deep enough to penetrate the water table, the height of the water measured in the well is called the piezometric head. Its amount is the sum of the elevation, z above some reference level, and the pressure head, $p_w/\rho g$, which depends on the water pressure and the density of the fluid, which account for the buoyancy force acting on the water.

Pizometric Head:

$$h(x,z) = z + \frac{p_w(x,z)}{\rho g} \tag{2}$$

The Poisson equation written in terms of hydraulic head is derived directly via the mass conservation principle. The term on the right hand side of the equation ζ, represents the sap flow rate and accounts for the water leaving the aquifer through ET. We will be interested in two particular values of sap flow: the minimum sap flow rate and the maximum sap flow rate, denoted by ζ_{min} and ζ_{max}, respectively.

Poisson's Equation:

$$\frac{\partial^2 h}{\partial x^2} + \frac{\partial^2 h}{\partial z^2} = -\frac{\zeta}{k} \tag{3}$$

In the schematic drawing of the aquifer above the stream bank is represented as a rectangle. There are two reasons for assuming that the stream is rectangular. First, there does not exist a practical or reliable method to determine the actual shape of the underlying bedrock layer. Second, if we take into consideration that in the stream banks in the Andrews we are focusing tend to be thin, that is, the length from the stream to the main channel boundary is longer than the depth of the aquifer, then it becomes plausible that the direction of flow is approximately parallel to the horizontal edge of the rectangle.

In order to extract a solution from the Poisson equation for this particular system it is necessary to prescribe various boundary conditions on the aquifer.

$$\begin{aligned} &h(0, z \le H) = H \\ &h(x,z) = z \\ &h(x,Z) = Z \\ &\frac{\partial h}{\partial x}(X,z) = 0 \\ &\frac{\partial h}{\partial z}(x,0) = 0 \end{aligned} \tag{I-V}$$

The boundary conditions I-II describe the piezometric head along the seepage surface between the aquifer and the stream. Condition I says that the piezometric head is equal to the stream height, H at points below the stage height of the stream. Condition II says that the piezometric head along the seepage surface above the stream is equal to the elevation, z. At the ground level the piezometric head is

equal to the depth of the aquifer, Z(III). This assumption comes from the fact that water pressure at the top of the column is zero, and so the piezometric head is reduced to the elevation, *Z*. Condition IV says that no water flows across the boundary and is a result of the impermeable underlying bedrock layer. Similarly, the final assumption(V) states the volumetric flux along the boundary of the main channel is zero[2].

Using the method of the Green's Function[4] to solve Poisson equation in the presence of the preceding boundary conditions we obtain the follow distribution of piezometric head in the ideal aquifer.

Piezometric Head given by the Solution to Poisson's Equation:

$$h(x,z) = Z - \left[\int_0^Z \frac{\partial}{\partial x} G_{(\eta,\vartheta)}(0,z-Z)\cdot h(0,z-Z)dz - \int_0^Z\int_0^X \frac{\zeta}{k}\cdot G_{(\eta,\vartheta)}(x,z-Z)dxdz)\right] \qquad (4)$$

(4)

Using the piezometric head in (4) above and Darcy's law we can estimate *q*, the discharge per unit length of the stream from adjacent riparian aquifers.

$$q = -k\cdot\int_0^Z \frac{\partial h}{\partial x}(0,z)dz = -k\cdot\left[\int_0^X \frac{\partial h}{\partial z}(x,Z)dz - \zeta XZ\right] \qquad (5)$$

The flow rate *q* can be converted to the stream discharge of any given length of the stream, *l*.

$$Q = 2q\cdot l \qquad (6)$$

Applications of the Model:

With this ideal aquifer model at hand, we hope to extract useful information about stream discharge predicted by the model. Keeping in mind the assumption that the volume of water leaving the aquifer as ET can be estimated from sap flow, we would like to implement the model described hitherto to test whether or not the model's predicted change in discharge is comparable to the actual daily change in discharge at the stream gauge. The minimum and maximum actual discharges of the stream are denoted respectively by $\overline{Q_{\min}}$ and $\overline{Q_{\max}}$. Labeling the minimum discharge predicted the model, Q_{min} and $Q_{\max}$. It is now straightforward to compare the predicted change in discharge, ΔQ to the actual minimum discharge at the stream gauge, $\overline{\Delta Q}$ from (7) and (8) below.

$$\Delta Q = Q_{\max} - Q_{\min} \qquad (7)$$

$$\overline{\Delta Q} = \overline{Q_{\max}} - \overline{Q_{\min}} \qquad (8)$$

It is also interesting in the context of this model to think of discharge in (5) from the aquifer as a function of the sap flow rate, ζ. Consider the following diagram showing several configurations of the piezometric surface in our idealized stream bank.

Diagram :

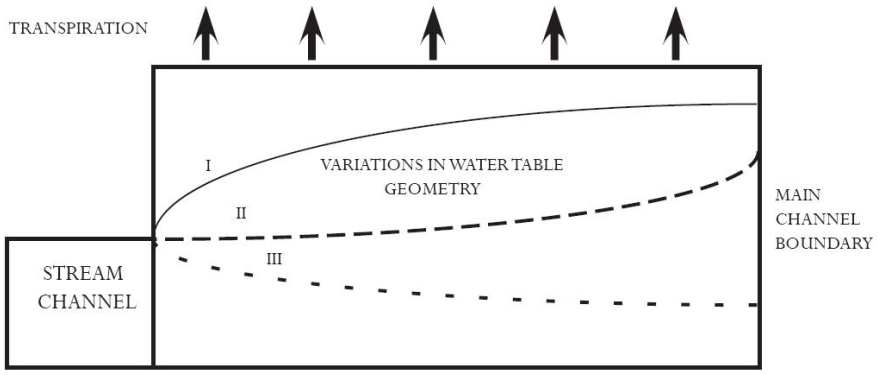

By varying the magnitude of ζ we would like to determine if this model predicts that the direction of flow from the model aquifer, given by Darcy's law, can change depending on the magnitude of ζ. That is, does there exist some threshold of ζ, at which water no longer leaves the stream bank, but instream leaves the stream and enters the stream bank. This is an interesting question because the existence of losing reaches along streams has been well observed and it is always a matter of interest in what ways a model comports with observations. If the threshold of ζ is within some reasonable physical range for sap flux values, then this model predicts some interesting results pertaining to hyporheic flow and the generation of losing reaches. The development of these losing reaches during acute periods of high sap flux could be strongly related to the underlying cause of the observed diel fluctuations.

Assuming the diel signal is local and additive over channel length, does sap flow in vegetated alluvial channel account for observed diel fluctuations at the stream gauge?

Objective

Previous work on the diel fluctuations in the HJ Andrews experimental forest has shown that there is a disparity between the amount of water lost to evapotranspiration from the whole watershed and the observed fluctuation at the stream gauge (Bond, 2002). By measuring sap flux density (the mass of sap moved by the tree in a day per area sapwood) and the area of sapwood per tree (the cross-sectional area of the tree that corresponds to sap movement, for which allometric relationships exist), the volume of water lost per day due to transpiration from all the trees in the entire watershed is significantly greater than the observed water loss at the stream gauge from the diel signal (Moore, 2004). In addition, existing

ideas about the generation of the diel signal suggest that it must be produced spatially local to the stream gauge in order for the signal to constructively interfere and produce an observable signal at the stream gauge. From our direct field observations using our staff gauge experiments, we showed that a diel signal is present far upstream in the channel and that all of the signals are in phase. The staff gauge experiments also demonstrated that bedrock channels appear to be much less able to communicate a diel signal than alluvial channel reaches. From this, we developed a hypothesis that all alluvial reaches contribute to the diel signal and no bedrock reaches contribute to the diel signal. Further, we wanted to know if evapotranspiration from vegetation growing only in the channel network would be capable of producing the diel signal observed at the stream gauge. To do this, we needed to find approximations for the volume of water lost to evapotranspiration at the stream gauge and a volume of water lost to evapotranspiration to see if the two values are comparable. In addition, we wanted to see if excluding trees based on the lithology of the reaches in which they are growing (based on our observations that alluvial diel signals are greater than bedrock signals) could still produce the signal at the stream gauge. From this, a better understanding of the interaction between lithological characteristics and diel signal production, as well as the spatial characteristics of the generation of the diel signal can be achieved.

Methods

This project synthesizes field observations, allometric relationships, and remote sensing (LiDAR) data to produce approximations for evapotranspiration (ET). During initial site surveys, we evaluated reaches of watersheds 1 and 2as either alluvium or bedrock. Within the alluvium category, we inferred that ET signal associated with trees growing in the channel would be manifested in overland flow because of the relatively high hydraulic conductivity of the sediment in the channel. In contrast, we reasoned that reaches that have carved down to bedrock with apparently little interaction with the hillslopes were non-communicative with the overland flow. For this investigation, only vegetation growing in the channel was considered. This approach is based on the assumption that hydraulic conductivity is too low in the hillslopes for a signal generated there to present itself in a daily signal from ET activity.

In ArcGIS, we identified and demarcated channels by producing a raster set of slopes from bare earth LiDAR data (*Figure 13*). All LiDAR data sets used are 1-meter resolution and was collected in 2008. Because hillslopes have a significantly steeper gradient than do channels, it was straightforward to identify the channel (*Figure 14*). The channel outline produced was verified by comparing it to existing HJ Andrews maps. From the geological survey data collected, the channel outline was broken up into reaches that we described as: 1) dry, 2) alluvium, 3) bedrock (no exchange expected), 4) bedrock channel with debris (wood, loose sediment, vegetation), or 5) extensive log jam (*Figure 15*).

We produced a raster of tree heights in ArcGIS from LiDAR by subtracting the bare earth dataset from the highest hits dataset to approximate the magnitude of vegetation in the channel (*Figure 16*). The only trees included in the survey were ones that were growing directly in the channel. To identify these, we selected only trees with an inferred centroid lying in the channel (*Figure 17*). After we identified all trees growing in any of the channel reaches, we broke the trees up into separate groups based on the lithological categorization of the reach in which they are growing. The groupings tested were: 1) all trees in all reaches of the channel, 2) all trees in non-dry channels, 3) bedrock channels with debris, alluvium, and log jams, or 4) only alluvium and log jam reaches.

We converted tree heights to sapwood area using allometric conversions. In watershed 1, we assumed all trees were red alder (*alnus rubra*) and that all trees in watershed 2 were old growth douglas

fir (*pseudotsuga menziesii*). Using species-specific allometric relationships (Richards, 1959; Garman, 1995), we converted tree heights to diameter at breast height (DBH). For *p. menziesii*, an allometric relationship between DBH and sapwood area was used to approximate sapwood area. For *a. rubra*, we used a linear relationship (produced from data in *Moore, 2004*) between diameter and sapwood area to approximate sapwood area. Sap flux densities for *a. rubra* and *p. mensiesii* were calculated in Moore, 2004 for a summer season in 1999 in HJ Andrews. To maintain some temporal consistency with our geological survey (conducted early to mid August), we used sap flux density from August 22, 1999 for the calculations.

Approximations of the water loss at the stream gauge were also taken from 24-hour data starting at 10PM, August 22, 1999. This period was chosen because it extends from a discharge minimum to the discharge minimum the next day to give one full wavelength of the signal. In the absence of a diel draw of water from evapotranspiration, we assume that the discharge would be nearly constant and at the same level as the peak of the diel signal. So, in order to find how much water is lost from diel drawdown, the area between a horizontal line crossing the peak of the signal and the diel curve was calculated (*Figure 18*). This area represents a volume of water per unit area in the watershed. For each combination of reaches for each watershed, the approximated volume of water lost was compared to the observed loss of water from the gauge and compared (*Figure 19*).

Results

For watershed 1, we identified two distinct types of reaches: alluvium and dry. The estimated water loss for all trees in the channel, including dry tributaries, overestimated observed values by about 63% whereas calculations for only channels of water overestimated by only about 28.5%. Watershed 2 exhibited all 4 combinations of channel type. As with watershed 1, the estimate from all trees in the channel was the worst configuration, overestimating by 149%. By eliminating dry channels, however, the estimate was only improved slightly, but still overestimated at 118% of the observed value. After eliminating bedrock channels where hyporheic exchange was inferred to be nonexistent, the estimate improved, but again overestimated by 79%. When only reaches with alluvium and log jamming were considered, the estimate improved dramatically and only overestimated by about 7.3%.

No signal in discharge can be produced in an area without overland flow so, the overestimation by dry reaches is unsurprising. Also, the overestimation from bedrock reaches with no apparent connection to the hillslopes corroborates our suspicion that these reaches cannot participate in diel signal production since they do not appear to have any exchange between the overland flow and water in the hillslopes. The dramatic reduction in error by also eliminating bedrock channels with debris in them seems to indicate that these reaches are also not participating in diel signal production even though some contain vegetation that appear to be drawing water directly from overland flow. The strong agreement between low error estimates in both watersheds and the inclusion of only reaches with alluvium seems to indicate that these reaches are the most important in terms of the production of the diel signal. Further, because all investigated configurations are overestimates, this exercise suggests that even less of the stream network is contributing.

A possible explanation for the overestimation is the dissipation of discharge in the surface flow near the headwaters. Only tributaries that were absolutely dry were labeled as such, however, noticeable flow reductions upstream were noted in the survey. It is possible that removing some of these low flow zones could improve the diel signal estimations.

Many possible sources of error are present in the approximations used to produce these results. Creating channel polygons and demarcating trees manually from the LiDAR data could have resulted in bias. We attempted to account for this, however, by creating the same features in several independent repetitions and looking for disparities between the repetitions. Error also exists in the allometric conversions as well as in the sap flux density data we used from previous studies.

This project does not offer absolute evidence in regards to deciding which channel characteristics produce diel signals. It does, however, test the validity of our field observations by comparing how well various lithologically defined sets of trees approximate the observed water loss at the stream gauge. The relationships between observed and approximated water lost strongly agree with the hypothesis that all alluvial reaches contribute to the diel signal and bedrock reaches do not. Furthermore, the error in the alluvium channel approximations may at least be partially explained by inattention to overland flow diminishment upstream and is a possible area of further investigation. What is most interesting about the results of this finding is that it suggests that solely the vegetation growing in the stream channel is capable of producing the entire diel signal and the invocation of hillslope vegetation is not required to explain the diel signal. It suggests that an alternative interpretation of "local generation" as described in Bond, 2002, to mean local with respect to the stream channel is a valid possibility.

Conclusions:

Briefly, looking back at our summer research as a whole, we came up with four main conclusions. The analysis of long-term data at HJA showed that air temperature and discharge time lags depend on watershed and antecedent precipitation. Our field work produced two findings. First, diel signals exist and are in phase up the stream network. Second, alluvial stage height fluctuations are greater than bedrock stage height fluctuations. Finally, through our watershed surveys and subsequent LiDAR data analysis we determined that vegetated alluvial channel area can produce the measured diel fluctuations observed at stream gage. In addition, we created an analytical model describing stream bank outflow as a function of ET in the riparian zone to further our conceptual understanding of diel fluctuations.

References:

A. D. Polyanin: Handbook of Linear Partial Differential Equations for Engineers and Scientists, Chapman & Hall/CRC, 2002

Barnard, H.R., Graham, C.B., Van Verseveld, W.J., Brooks, J.R., Bond, B.J., and McDonnell, J.J. 2010. Mechanistic assessment of hillslope transpiration controls of diel subsurface flow: a steady-state irrigation approach. *Ecohydrology.* **3**: 133–142

Blaney, H.F., Taylor, C.A., Young, A.A., 1930. Rainfall penetration and consumptive use of water in the Santa Ana River Valley and Coastal Plain. California Department of Public Works, Division of Water Resorces, Bulletin 33, 162pp.

Bond, B.J., Jones, J.A., Phillips, N., Post, D., and McDonnell, J.J. 2002. The zone of vegetation influence on baseflow revealed by diel patterns of streamflow and vegetation water use in a headwater basin. *Hydrol. Process.* **16**: 1671–1677

Bousek, R., 1933. Das tägliche periodische Steigen und Fallen des Grundwasserspiegels. Die Wasserwirtschaft 31, 427–429.

Brusaert W.: Hydrology, An Introduction, Cambridge University Press, 2005

Clark, J. 2007. Models for Ecological Data: An Introduction. Oxford University Press.

Dunford, A.R., Fletcher, P.W., 1947. Effect of removal of streambank vegetation upon water yield. Transactions, American Geophysical Union 28, 105–110.

Garman, Steven L., Acker, Steven A., Ohmann, Juliet L., Spies, Thomas A. 1995. Asympytotic Height-Diameter Equations for Twenty-Four Tree Species in Western Oregon. Forest Research Laboratory, Oregon State University. Research Contribution 10

Gribovszki, Z., Kalicz, P., Szilágyi, J., Kucsara, M., 2008. Riparian zone evapotranspiration estimation from diurnal groundwater level fluctuations. Journal of Hydrology 349 (1–2), 6–17.

Gribovski et al. 2010. Diurnal fluctuations in shallow groundwater levels and streamflow rates and their interpretation- A review, *Journal of Hydrology*. **385**: 371-381.

Guenther R. and J. Lee: Partial Differential Equations of Mathematical Physics and Integral Equations, Dover Publications, 1988

Moore, G.W., Bond, B.J., Jones, J.A., Phillips, N., and Meinzer, F.C. 2004. Structural and compositional controls on transpiration in 40- and 450-year-old riparian forests in western Oregon, USA. Tree Physiology **24**:481–491

Richards, F.J. 1959. A flexible growth function for empirical use. Journal of Experimental Biology 10:290-300.

Turner, David P., Acker, Steven A., Means, Joseph E., Garman, Steven L. 1999. Assessing alternative allometric algorithms for estimating leaf area of Douglas-fir trees and stands. *Forest Ecology and Management*. **126**:61-76

White, W.N., 1932. Method of Estimating Groundwater Supplies Based on Discharge by Plants and Evaporation from Soil – Results of Investigation in Escalante Valley. Tech. Rep., Utah – US Geological Survey. Water Supply Paper 659-A.

Wicht, C.L., 1941. Diurnal fluctuation in Jonkershoeckstreams due to evaporation and transpiration. Journal of the South African Forestry Association 7, 34–49.

Wondzell SM. 2006. Effect of morphology and discharge on hyporheic exchange flows in two small streams in the Cascade Mountains of Oregon, USA. *Hydrological Processes* **20**(2): 267 – 287, DOI: 10.1002/hyp.5902.

Wondzell SM, Gooseff MN, McGlynn BL. 2007. Flow velocity and the hydrologic behavior of streams during baseflow. *Geophysical Research Letters* **34**: L24404, DOI:10.1029/2007GL031256.

Wondzell et al 2010. An analysis of alternative conceptual models relating hyporheic exchange flwo to diel fluctuations in discharge during baseflow recession. Hydrological Processes 24, 686-694.

Note: The following is a draft of Nathaniel's section. To be incorporated when writing is complete.

(Nathaniel Gustafson – 20 August 2010)

Objectives

The HJ Andrews has collected an immense amount of data over the past several decades as part of its LTER (Long-Term Environmental Research) mission. In this project, we utilized this long-term data to help understand the source and nature of streamflow diel fluctuations.

Because so much data was available to study in a relatively short study period, the methods used to explore it were primarily involved free-form, flexible data exploration. This would allow interesting features that emerged in the data to be pursued more easily than a more rigidly scheduled effort might allow. The focus of this study was not to extract a rigorous quantitative model so much as to indentify interesting and potentially pertinent features of data associated with diel signals. By doing so, we hoped to identify some of the key watershed characteristics and seasonal variables which affect diel signal presence and strength.

We collected the inferences made from these observations into a Hierarchical Bayesian Model, using those described by Clark [1] as a guide. The resulting model is described in the results section.

Methods

The data explored primarily included discharge, solar radiation, and precipitation across all watersheds in the HJ Andrews (Watersheds 1, 2, 3, 6, 7, 8, 9, 10, and Mack Creek) for the years 2001 to 2009 (inclusive). Stream and air temperature were also occasionally explored as potential indicators of streamflow diel fluctuations.

The statistics package R was used to visualize and explore the data. Typically, exploring a year or set of years would lead to visual recognition of interesting features, which would lead to closer inspection. The plots which led to the features discussed below are included in the appendix. Also, because discussion of these patterns is difficult (if not meaningless) without the visuals, further descriptions of the features leading to the findings below are included with the figures in the appendix.

Results

Notable Patterns

Based on observation of a few key watersheds within the HJ Andrews Experimental Forest, some noteworthy patterns have been discovered, from which we make the following propositions:

- There are two main sources of diel signals: **Evapotranspiration**, and **Snowmelt**.
- A given watershed may exhibit one or both, or neither, at different magnitudes, depending on that watershed's spatial and qualitative characteristics.
- For **Evapotranspiration** (ET) signals:
    - The diel signal strength (measured in *volume of water lost per day*) is roughly proportional to Solar Radiation for that same day.
    - The signal is most clearly observable when there is no precipitation, but precipitation itself does not directly affect diel fluctuation.

- Discharge generally peaks around the *morning* hours.
- This signal is usually present when solar radiation becomes strong enough (about May) and remains until either the watershed has sufficiently drained (~August) or the dominant deciduous vegetation has discarded its leaves and ceased transpiring (Fall).

- For **Snowmelt** signals:
  - Discharge generally peaks around the *afternoon* hours (out of phase with ET-induced diel signals).
  - There is a strong correlation of diel signal strength to air temperature.
    - Due to time required for heat transfer, there is a lag between when air temperature increases and snow beings melting (inducing the signal).
    - This lag time may take a few days (as in early spring) or less (later spring).
  - Snowmelt signals begin showing up intermittently during warm phases in early spring, and taper off until early summer, once all snow has melted.

Hierarchical Bayesian Model

Conceptual models, such as that built here, can be made at any level of simplicity or complexity. The model used here attempts to capture some of the dynamics of both ET-related and snowmelt-related diel signals, along with their conditional dependence on groundwater and snow, respectively. It also recognizes that watersheds may differ significantly in the signals they exhibit; two watersheds of comparable size and even similar topography may differ significantly in signal strength, or one may exhibit a snowmelt-induced signal without an ET-induced signal, or vice versa. While there is some evidence that steeper watersheds, and those with stands that transpire more per hectare (such as Red Alder) seem to exhibit stronger ET-induced diel signals, data for many more watersheds would need to be collected before much could be said explicitly.

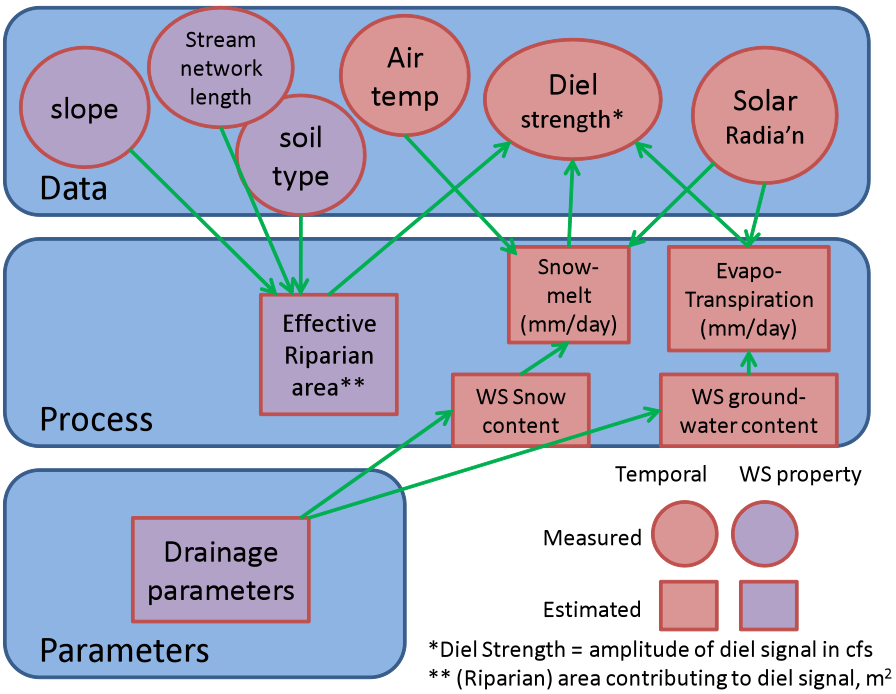

fig. 1 describes the resulting (Bayesian) model.

This model is not a Hierarchical Bayesian Model *per se*, but it gives the framework for which additional quantitative data can be used to train and parameterize the relations between items and potentially further elucidate the dynamics of diel signals.

Some of the discoveries in this project could serve as a general basis for defining these parameters – For example, seasonal timing generally allows for ET-related Diel signals from about May through August and snow-related signals about April til June, and ET-related signals for a given watershed are strongly correlated to Solar Radiation while snowmelt-related signals are more closely related to air temperature. Further refinement would be needed to quantify these parameters appreciably.

Future Work

The Hierarchical Bayesian Model constructed herein is conceptual, and has not yet been explicitly quantified with either parametric or empirical descriptors. Defining the relations between objects in the model quantitatively could increase the model's usefulness in describing the dynamics of diel signals.

One potentially helpful method could be collecting day-to-day average temperature or solar radiation data, and forming regression curves matching those to diel signal strength (including variance/error). Another could be collecting such data from many more watersheds exhibiting diel signals. The U.S. Geological Survey provides hourly discharge data for dozens of large- and small-scale watersheds in Oregon, as does the LTER network (*lterweb.org*). While the LTER network provides at least a few basic characteristics for the few dozen watersheds it is associated with across the U.S., the USGS does not. However, they can potentially be inferred from GIS analysis.

References

[1] Clark, J.S. and Gelfand, A.E. *Hierarchical Modelling for the Environmental Sciences: Statistical Methods and Applications*. 2006. Oxford.

Appendix

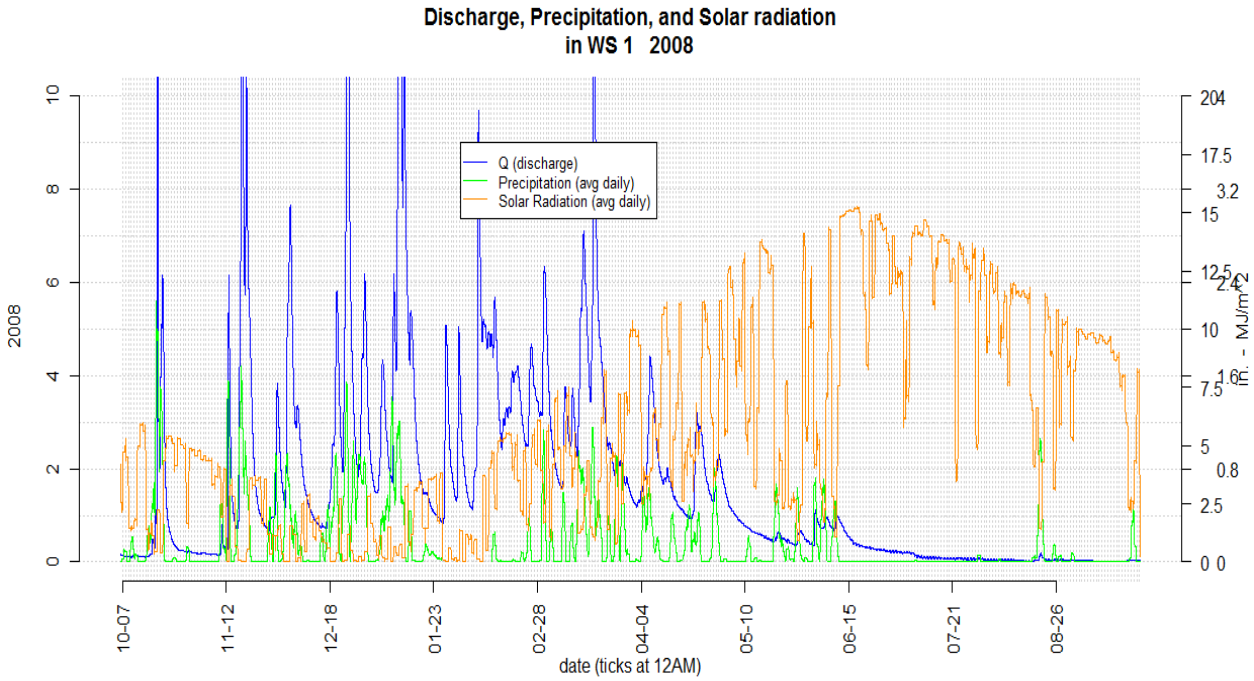

Fig. 2: Discharge, Solar Radiation, and Precipitation for watershed 1 in 2008. See Fig. 2

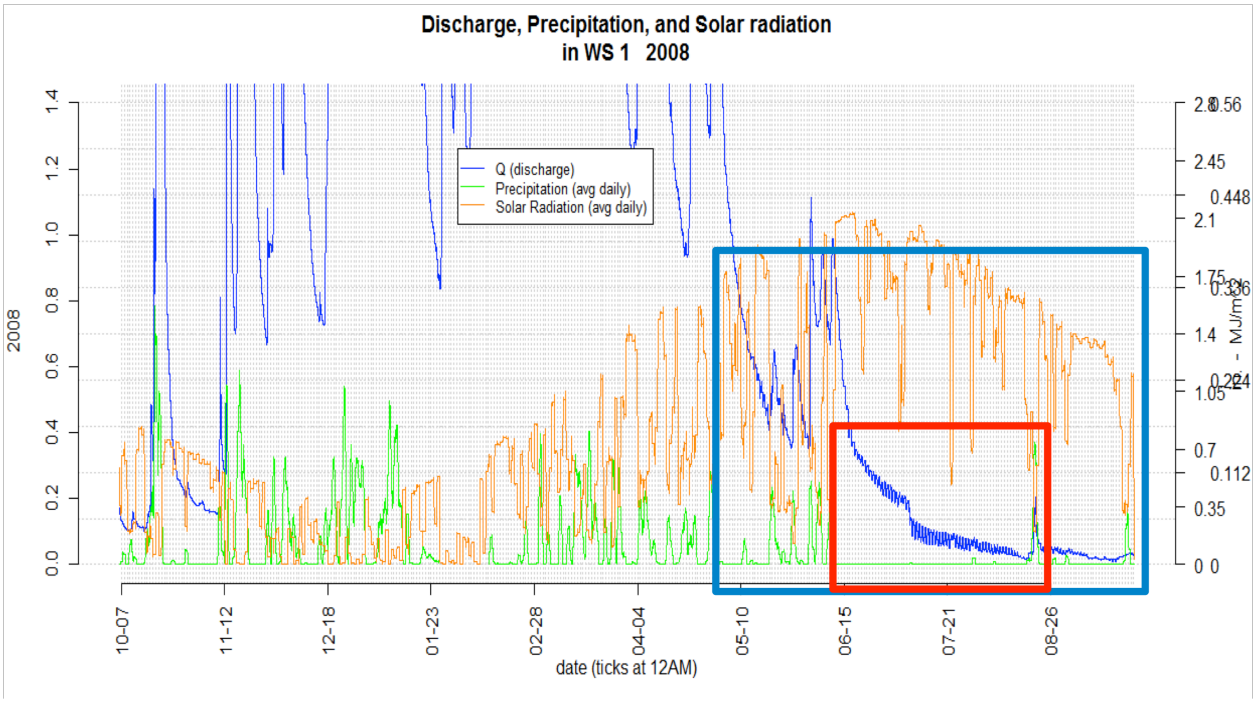

Fig. 3: Similar to figure 1, with discharge scaled to show summer diel fluctuations.

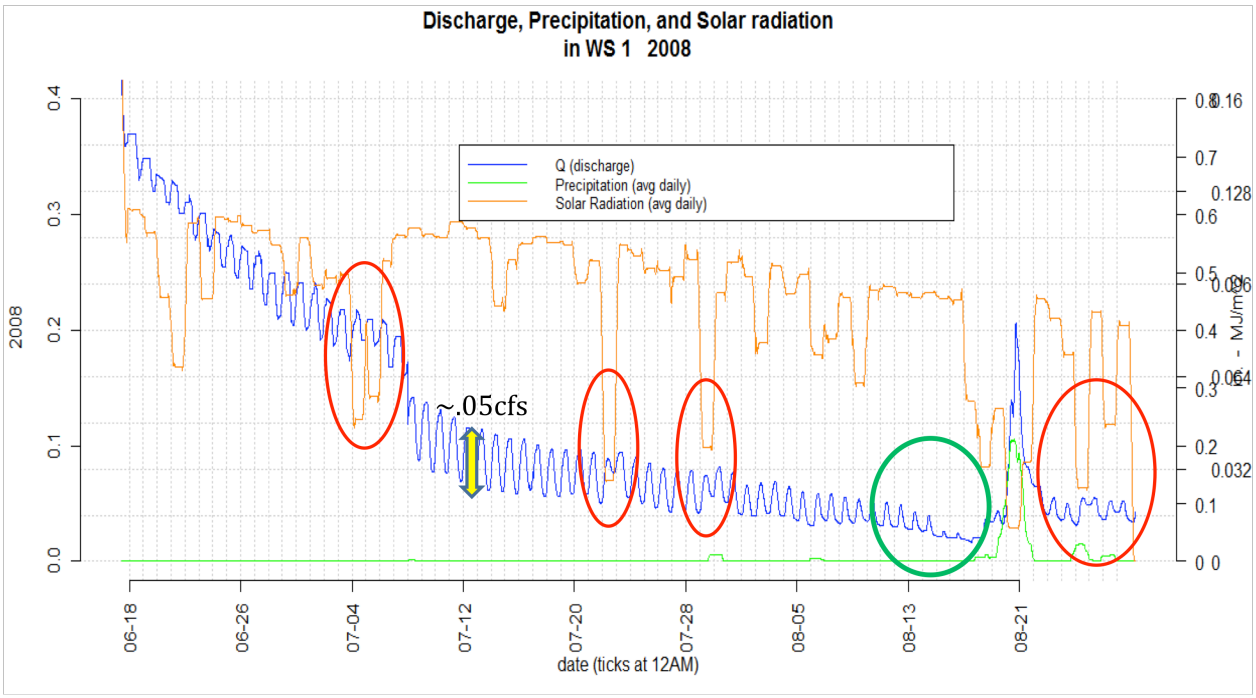

Fig. 4: A few interesting features are demonstrated here: The **red** circles indicate occurrences of cloudy days (with no significant precipitation) wherein a reduction in solar radiation seems very directly coupled to a reduction in signal strength for the associated days. Additional testing could be done to verify that this relationship is proportional. A one-to-one correspondence is clear between cloudy days and a reduction in signal strength, especially in the alternating sunny-cloudy days of the right red circle. The **green** circle highlights the diminishing of the summer diel signal – As progressively more groundwater drains out of the watershed, discharge recovery becomes narrower and shorter, discharge being recovered later into the morning and for a shorter time, until the signal essentially flattens out. This extending of the low phase could possibly be due to a hydraulic pressure deficit in trees, drawing water later and later into the night to replenish that lost during daytime transpiration. As groundwater becomes drier, trees will take additional time each day to restore that deficit.

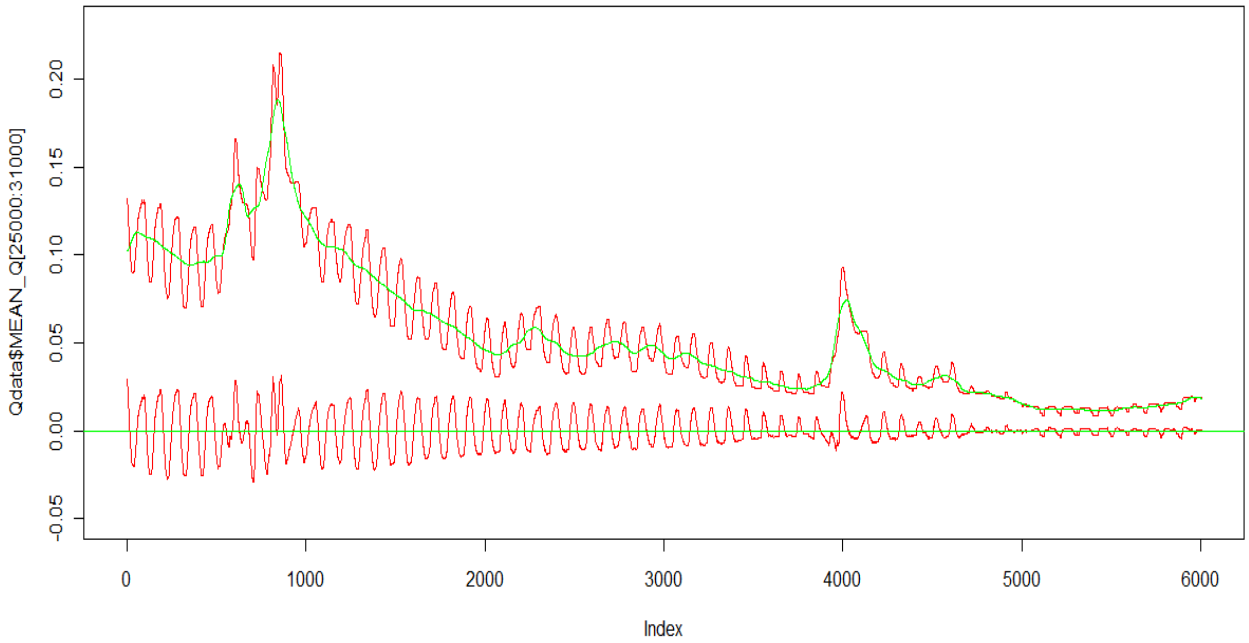

Fig. 5: A short example to illustrate subtracting the daily mean from discharge to highlight re residual diel signal.

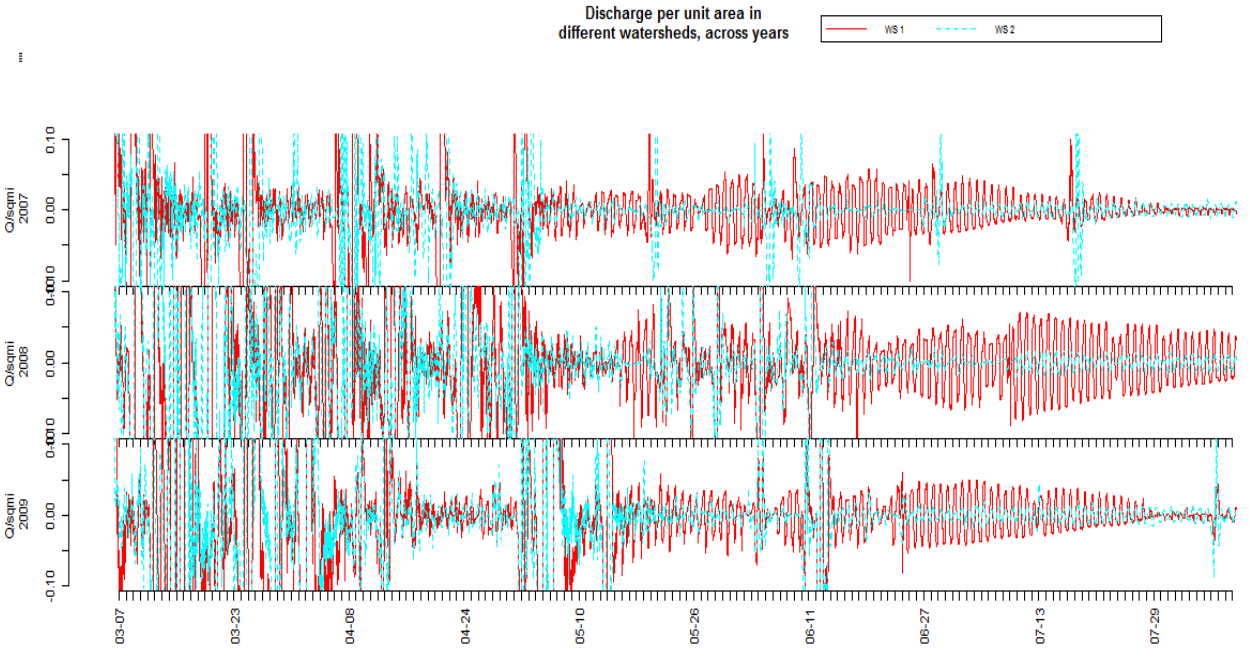

Fig. 6: Another example of residual diel signals. Watershed 1 shows an evident diel signal, starting as early as the beginning of May and increasing in strength before it diminishes as the watershed dries out for that year.

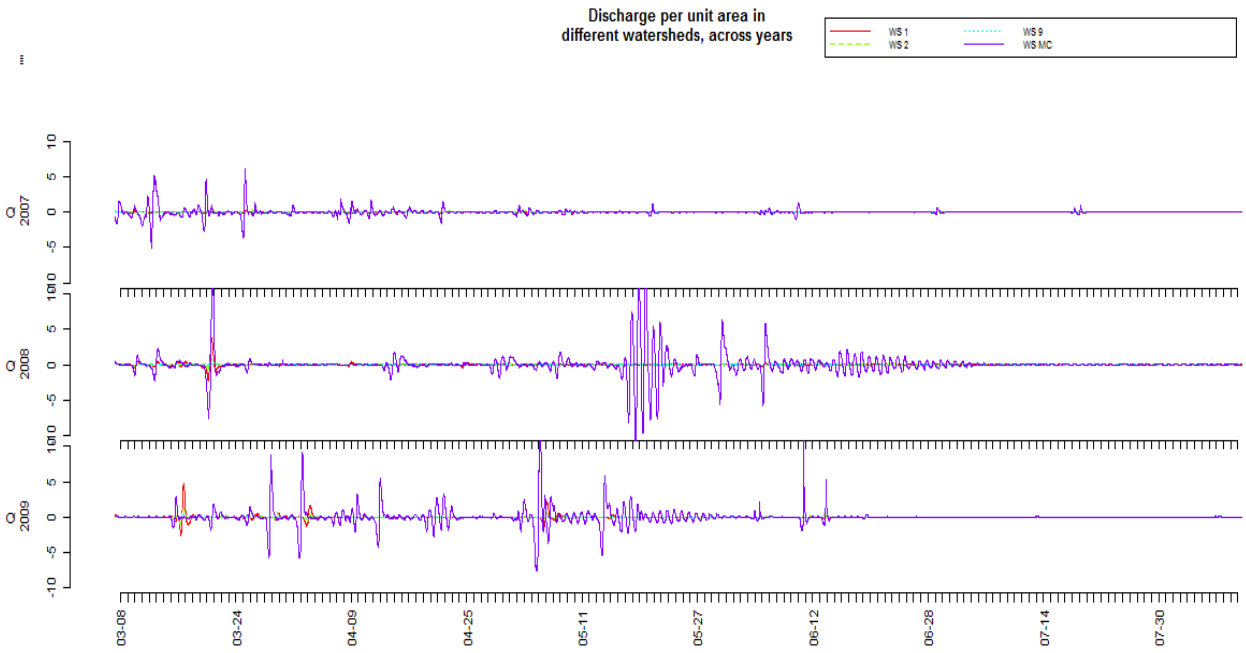

Fig. 7: Plotting residuals for Mack Creek*, strong diel signals are intermittently present. The large signal in May of 2008 is on the order of 20 cfs, 100 times larger than the comparable and more regular signal visible in WS1 in Figure 6. Also, this signal has a phase inverse to the ET-related signal evident in WS1, i.e. peaking discharge in the evening and minimum in the morning. See Figures 8-10. *Mack Creek is another watershed in the Andrews, roughly 10 times the size of WS1

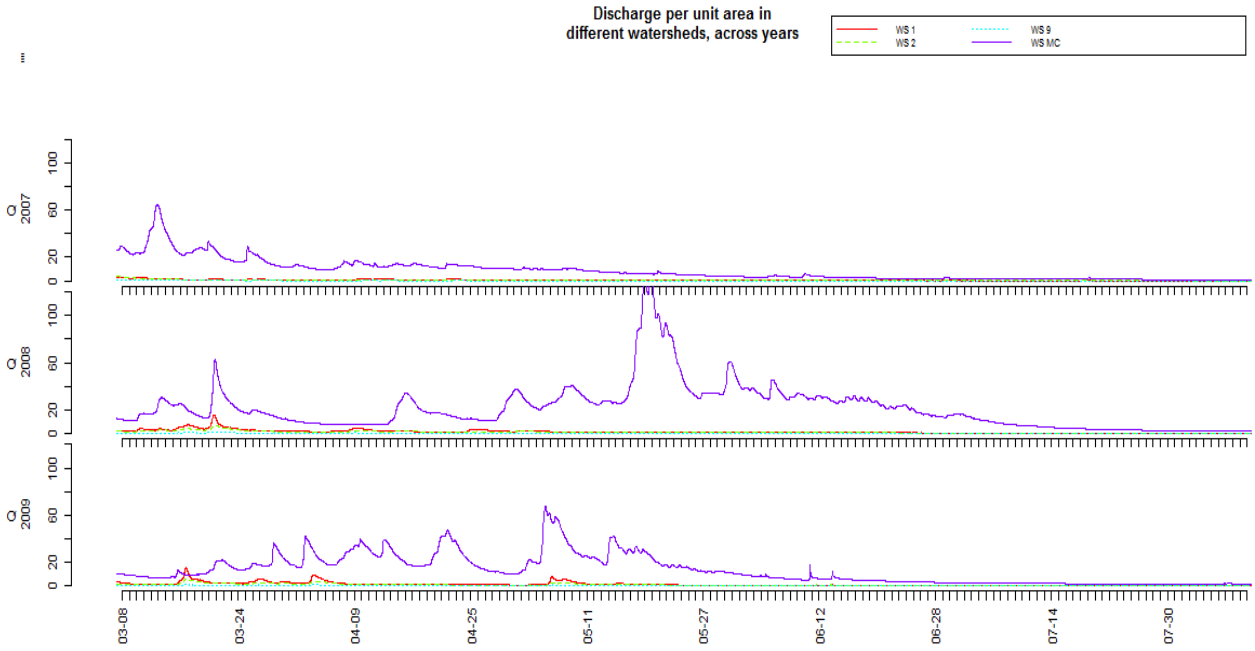

Fig. 8: Raw discharge for Mack Creek in the same time period shown in Figure 7. There are notable increases in discharge associated with diel signal pulses in Figure 7. See also Figures 9 and 10.

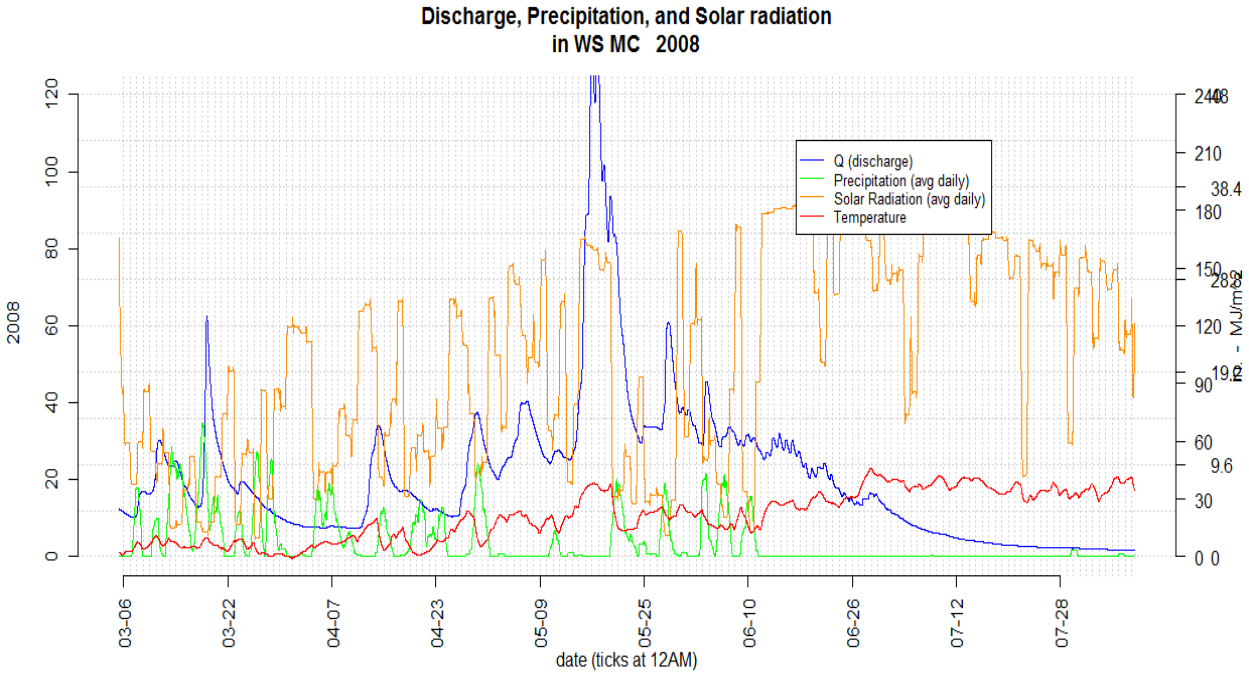

Fig. 9: There was no precipitation to drive the discharge pulse shown in figure 8 or the associated diel signal in Figure 7. There was, however, an uncharacteristic series of sunny days.. Another series of sunny days in late March failed to yield a similar signal, however, this signal does continue through June. Snowmelt would seem to be the primary cause of these signals. This would also be in line with the phase, which peaks in the evening, as opposed to ET-related signals such as those in WS 1, which peak in the morning. Temperature is shown as a potentially stronger correlate to snowmelt signals than solar radiation. See Figure 7-10.

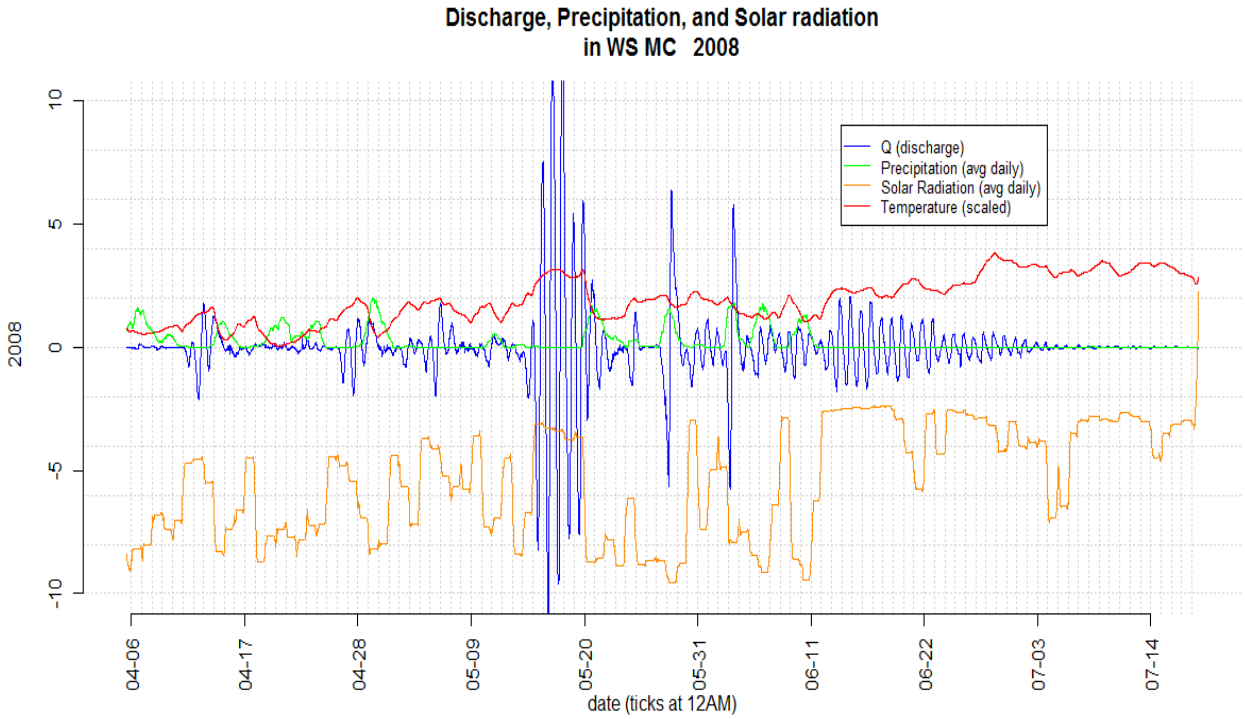

Fig. 11: The association between temperature and diel signal pulses. As a series of warm days heats up snow enough to being to melt, a snowmelt-related diel signal appears until precipitation or cooling halt it. Temperature seems to be a stronger indicator of snowmelt-related diel signals than solar radiation. As snow is melted off in June, this signal disappears. (Solar radiation here offset by -10 to avoid clutter) See Figures 7-9.

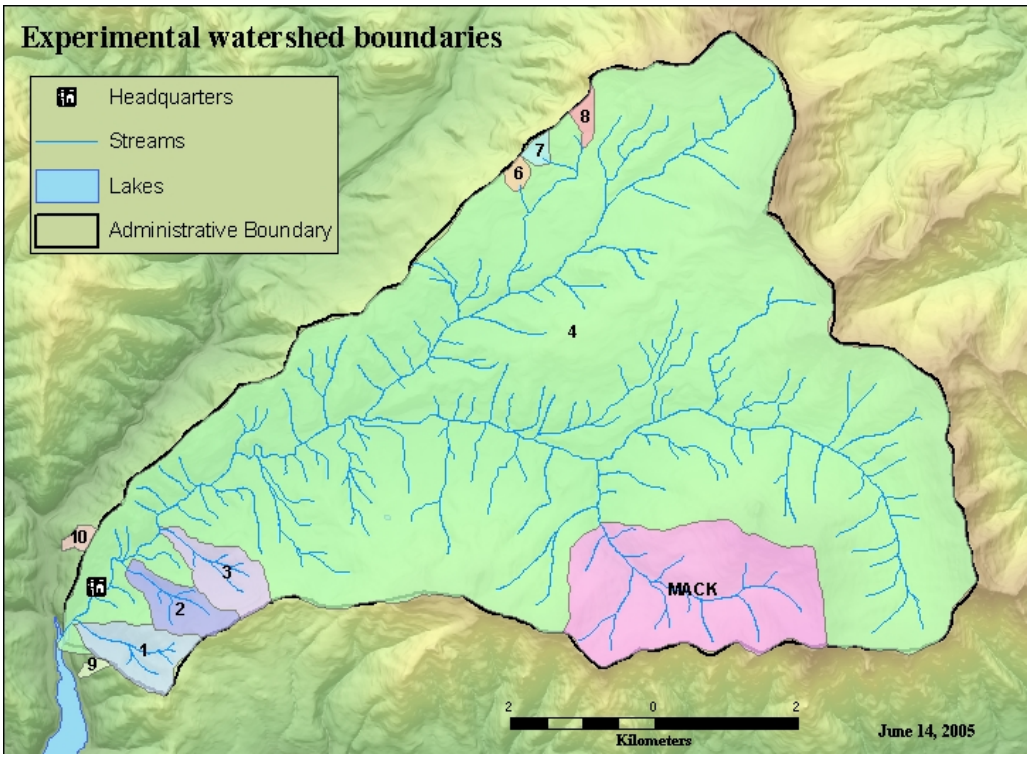

Figure 1

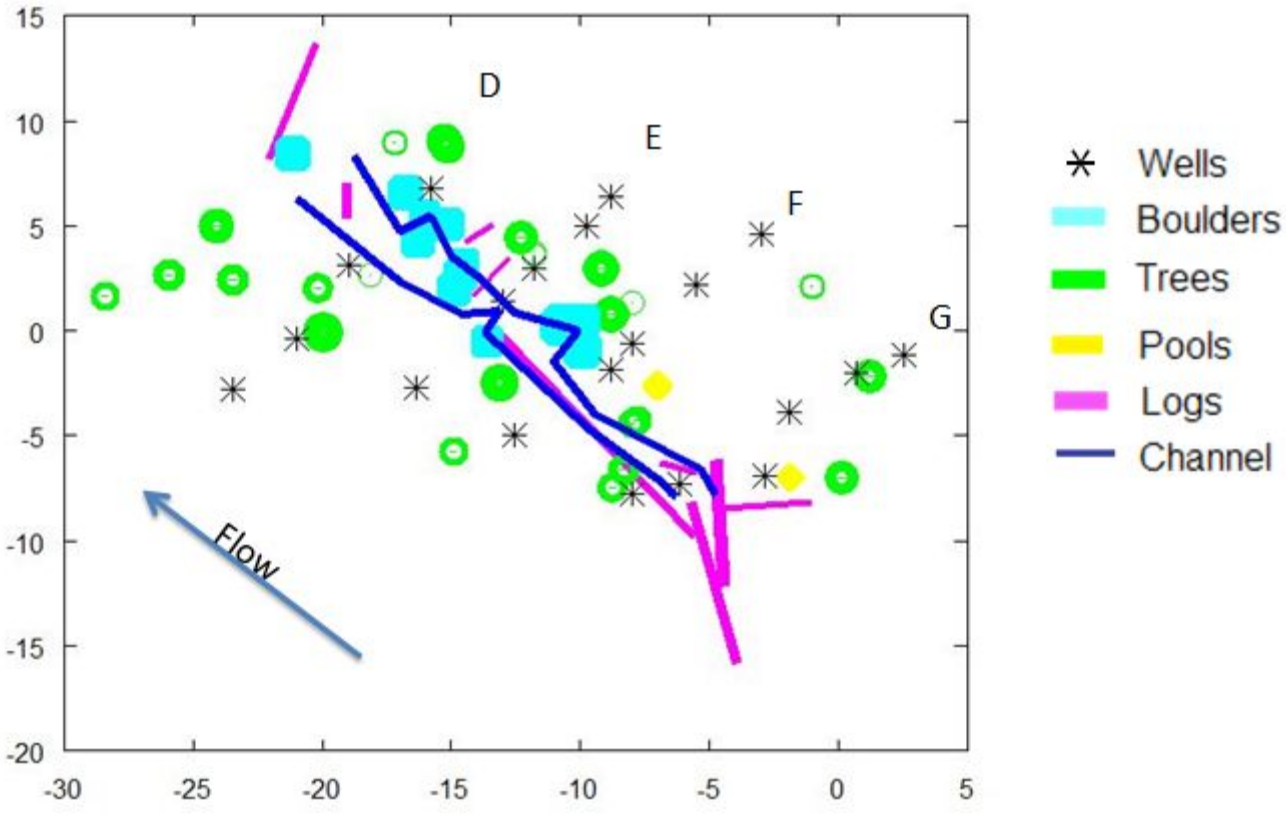

Figure 2

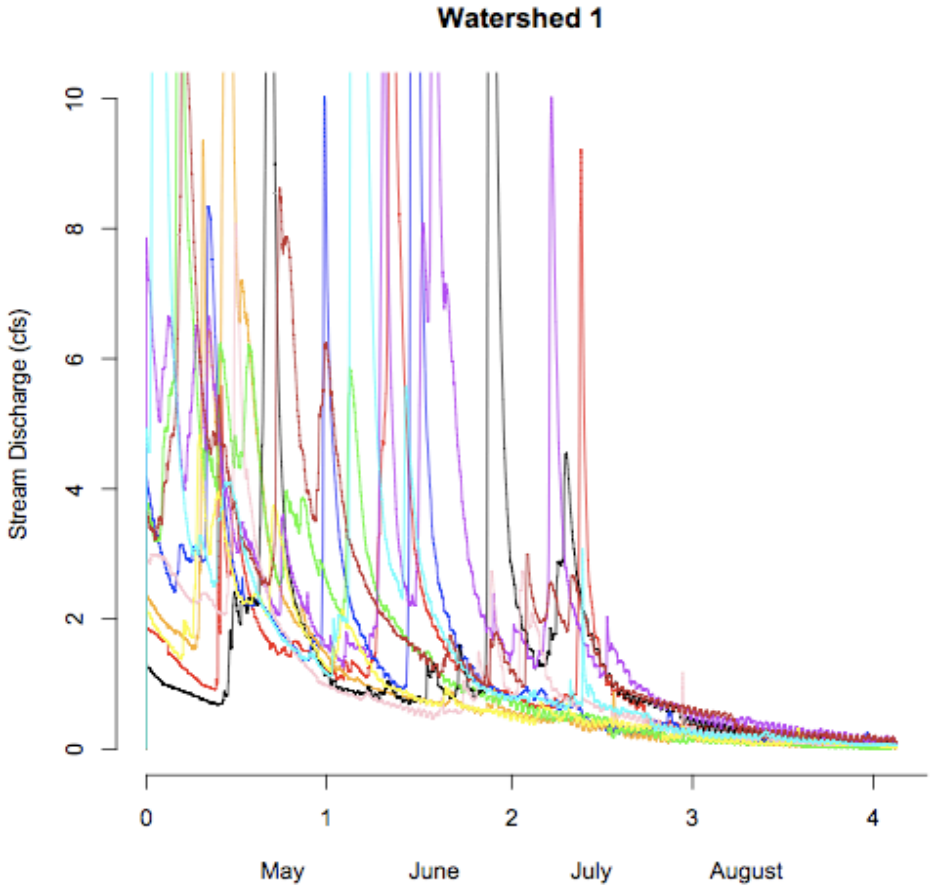

Figure 3

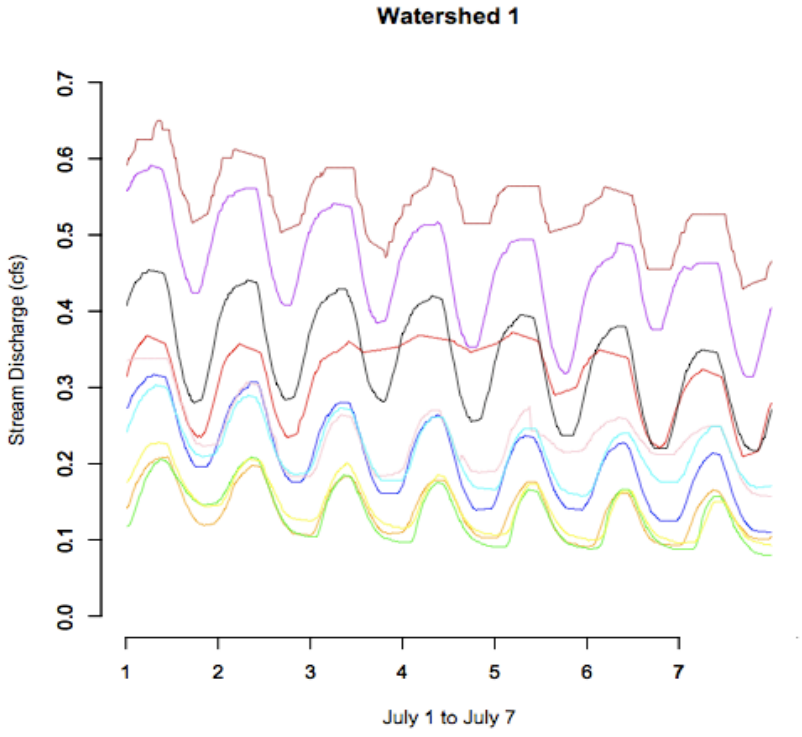

Figure 4

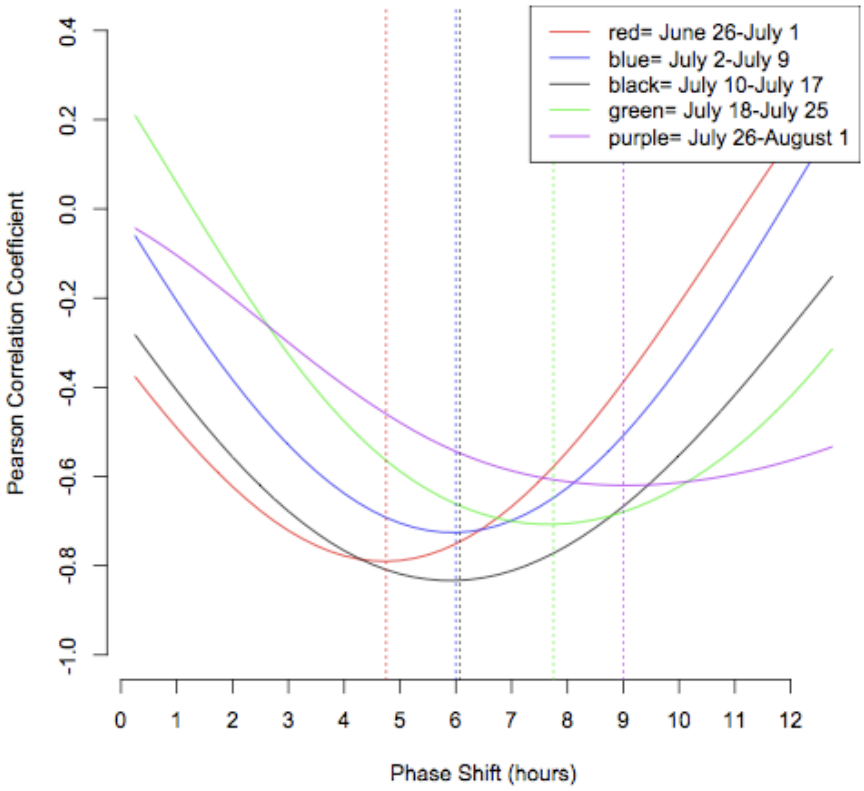

Figure 5: Watershed 1

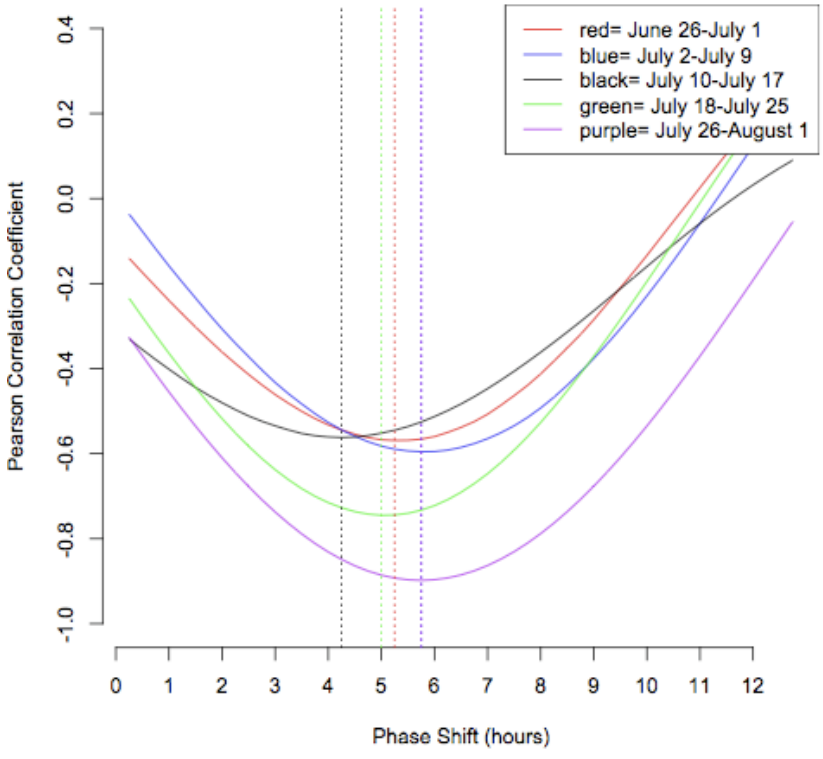

Figure 6: Watershed 9

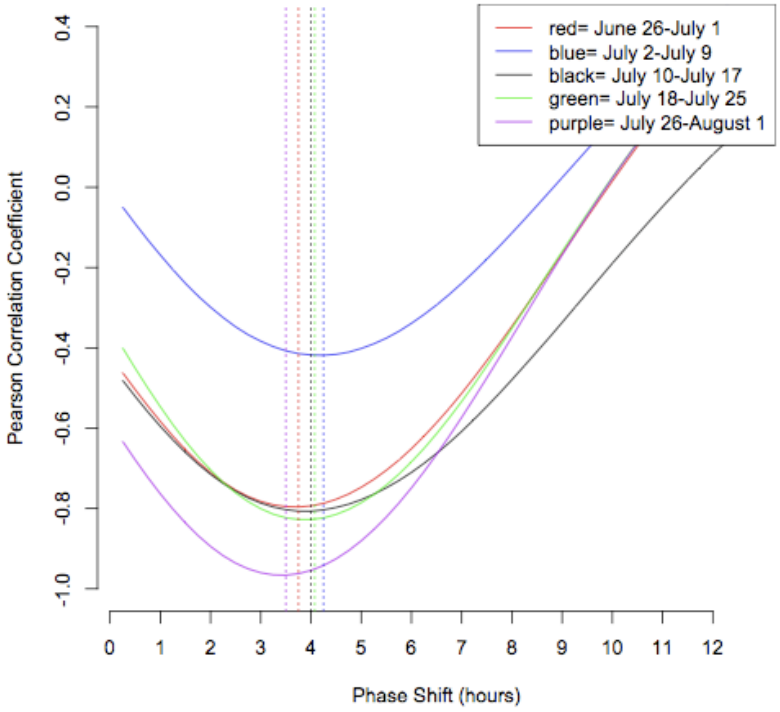

Figure 7: Watershed 10

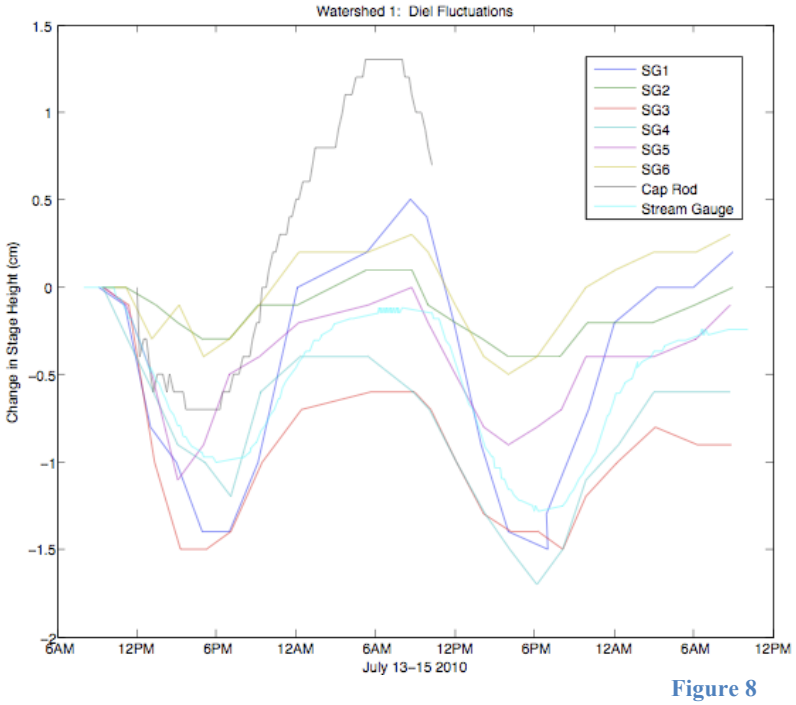

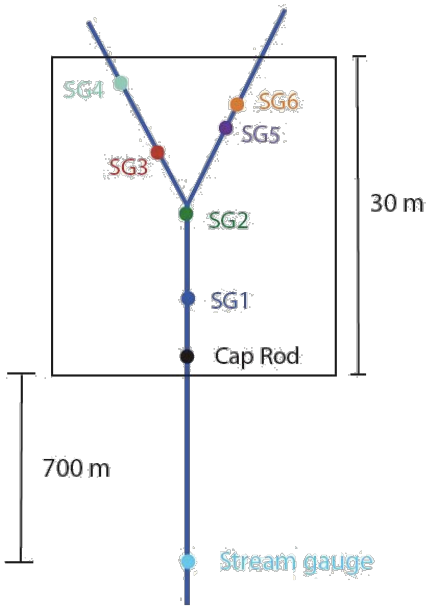

Figure 8

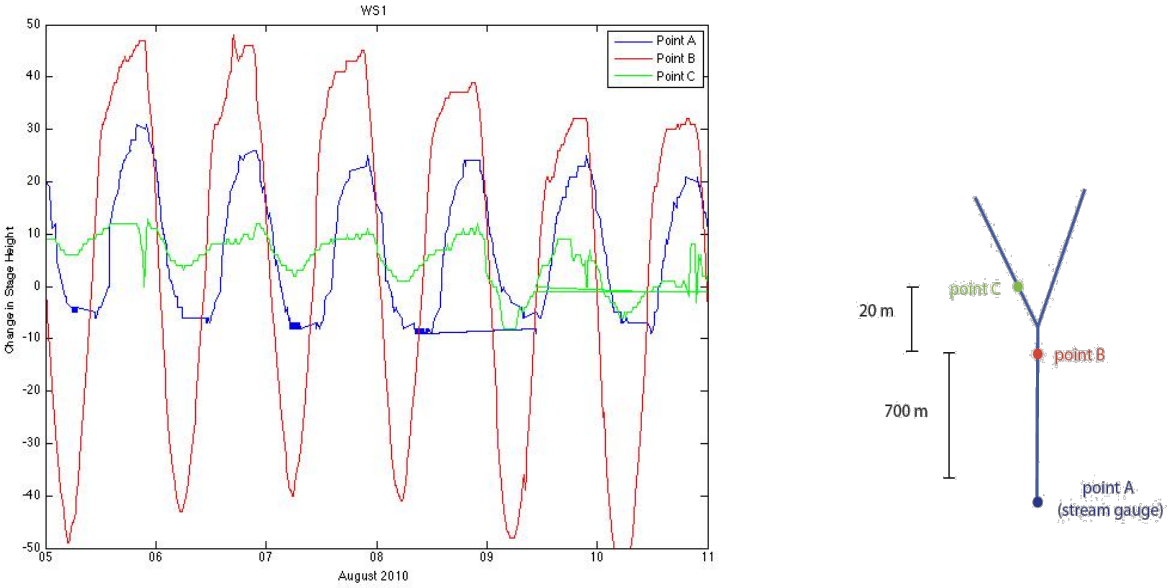

Figure 9

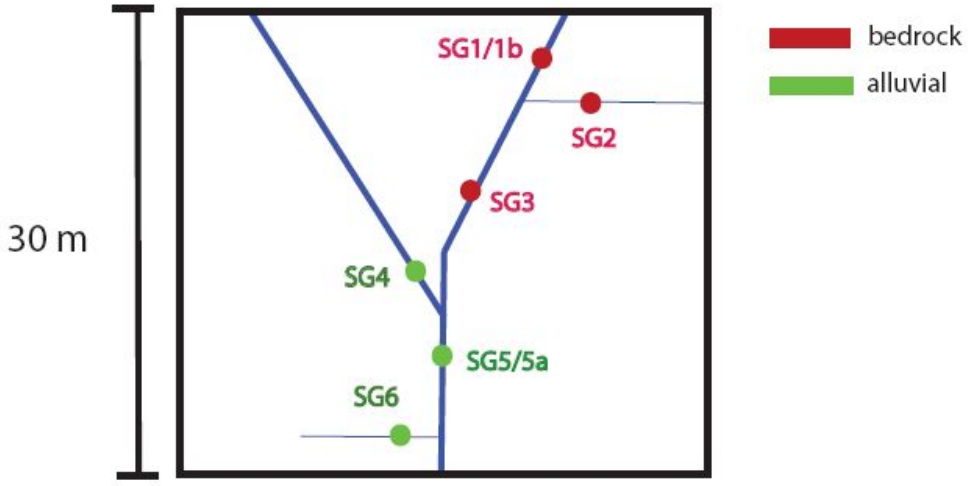

Figure 10

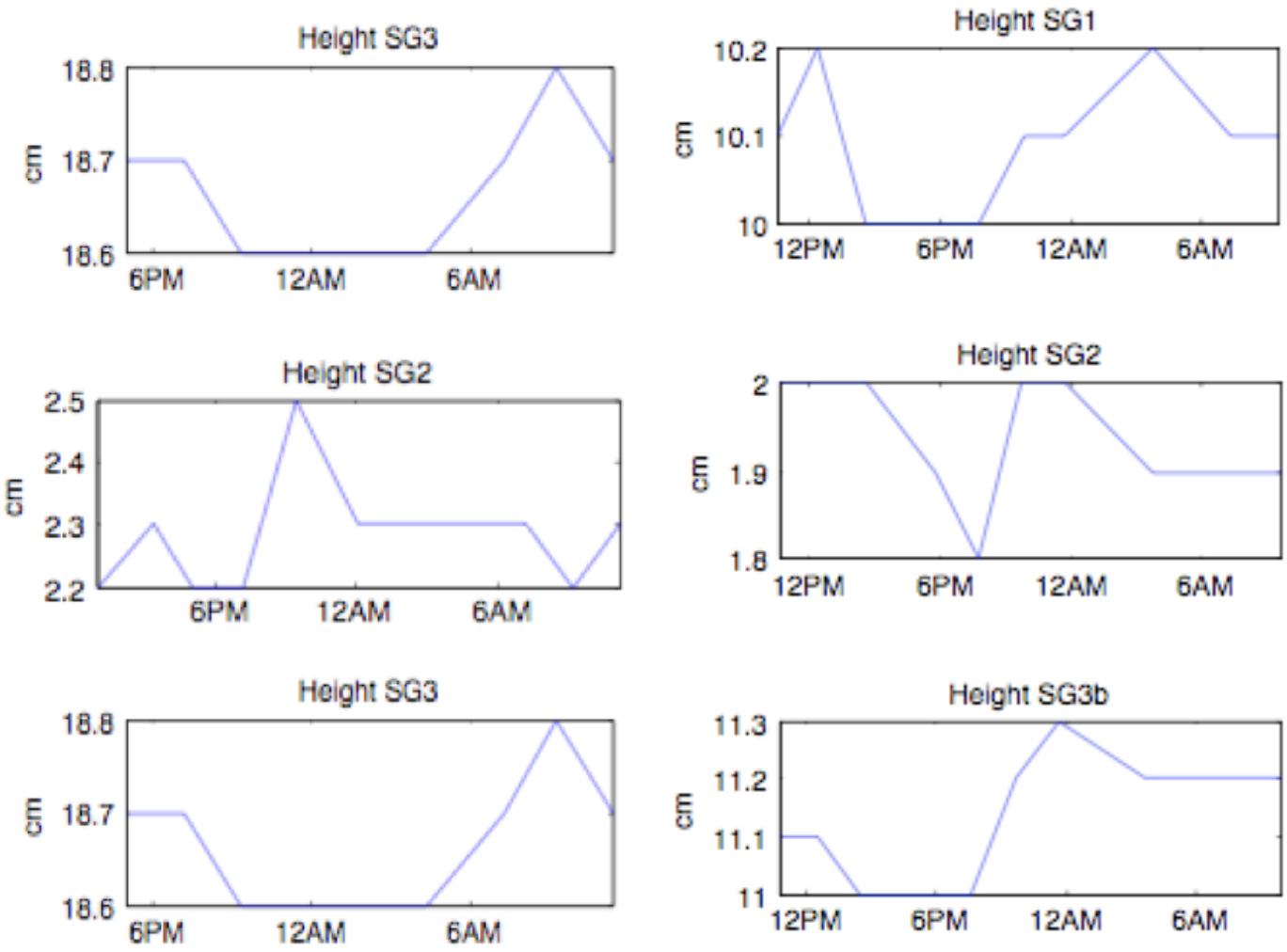

Figure 11: Bedrock channel staff gages (*Left:* July 7-8, 2010; *Right:* July 14-15, 2010)

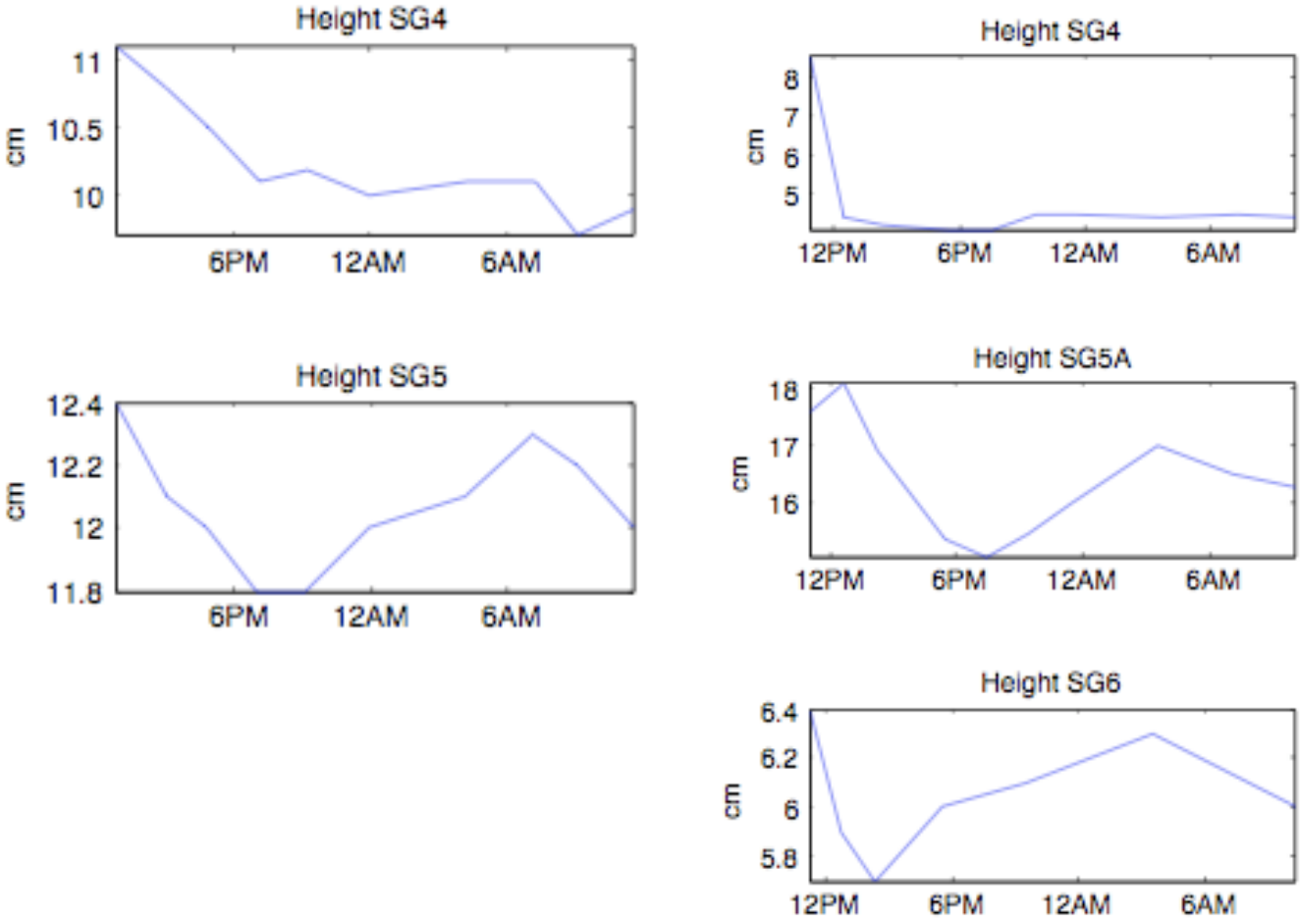

Figure 12: Alluvial channel staff gages (*Left:* July 7-8, 2010; *Right:* July 14-15, 2010)

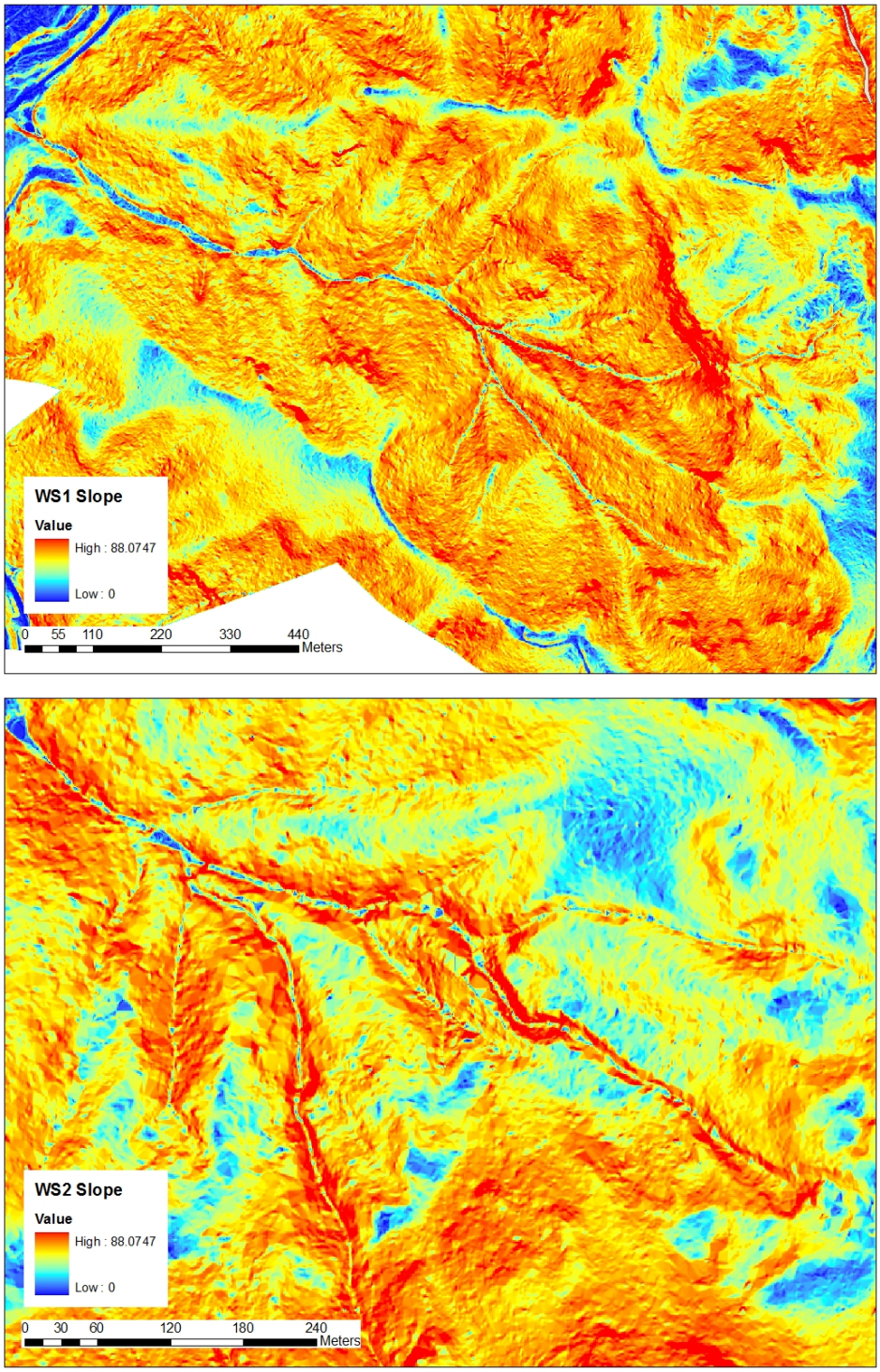

Figure 13: Slopes for watersheds 1 and 2

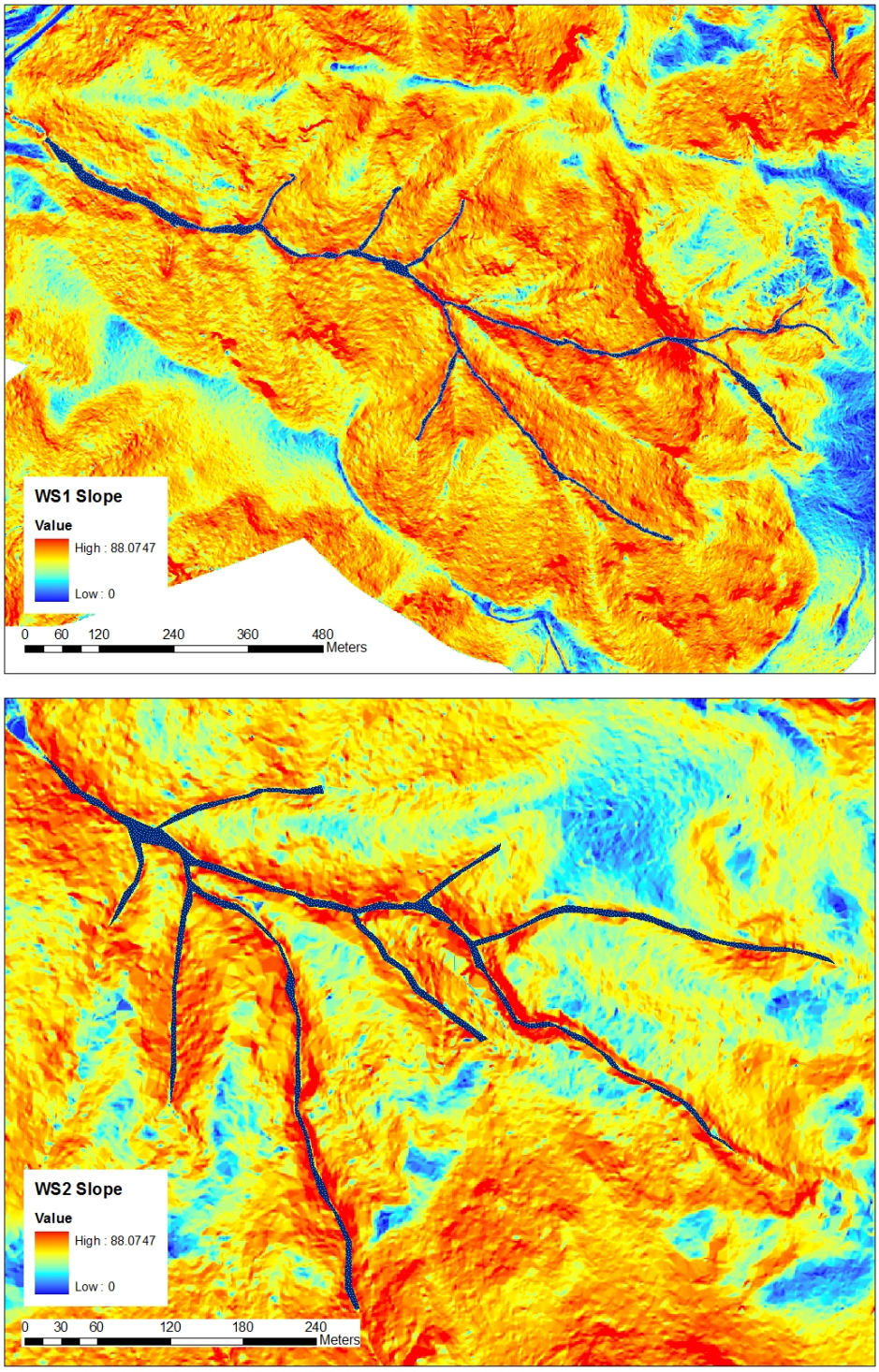

Figure 14: Inferred channel for watersheds 1 and 2

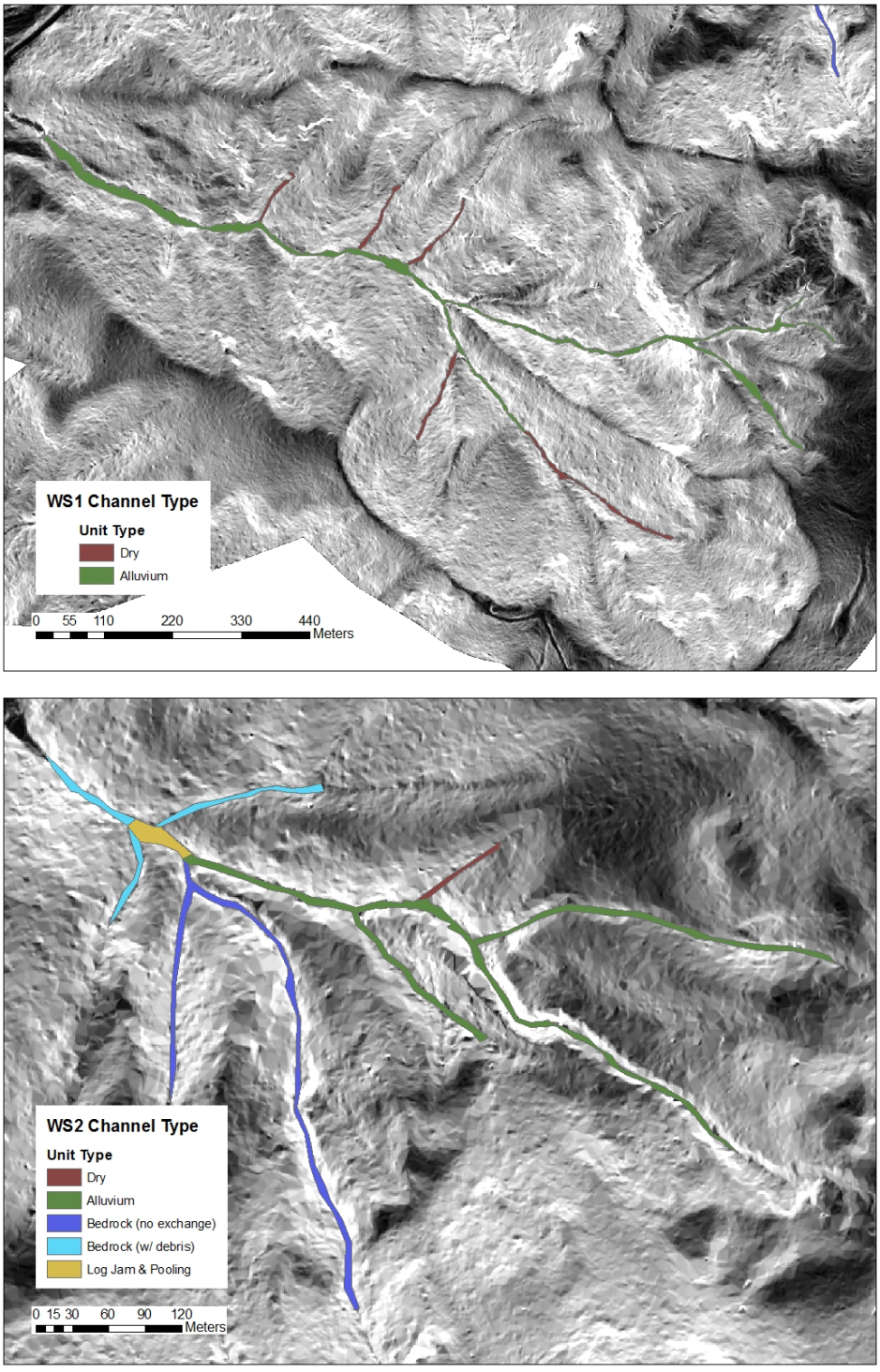

Figure 15: Channel type demarcation from geological survey for watersheds 1 and 2

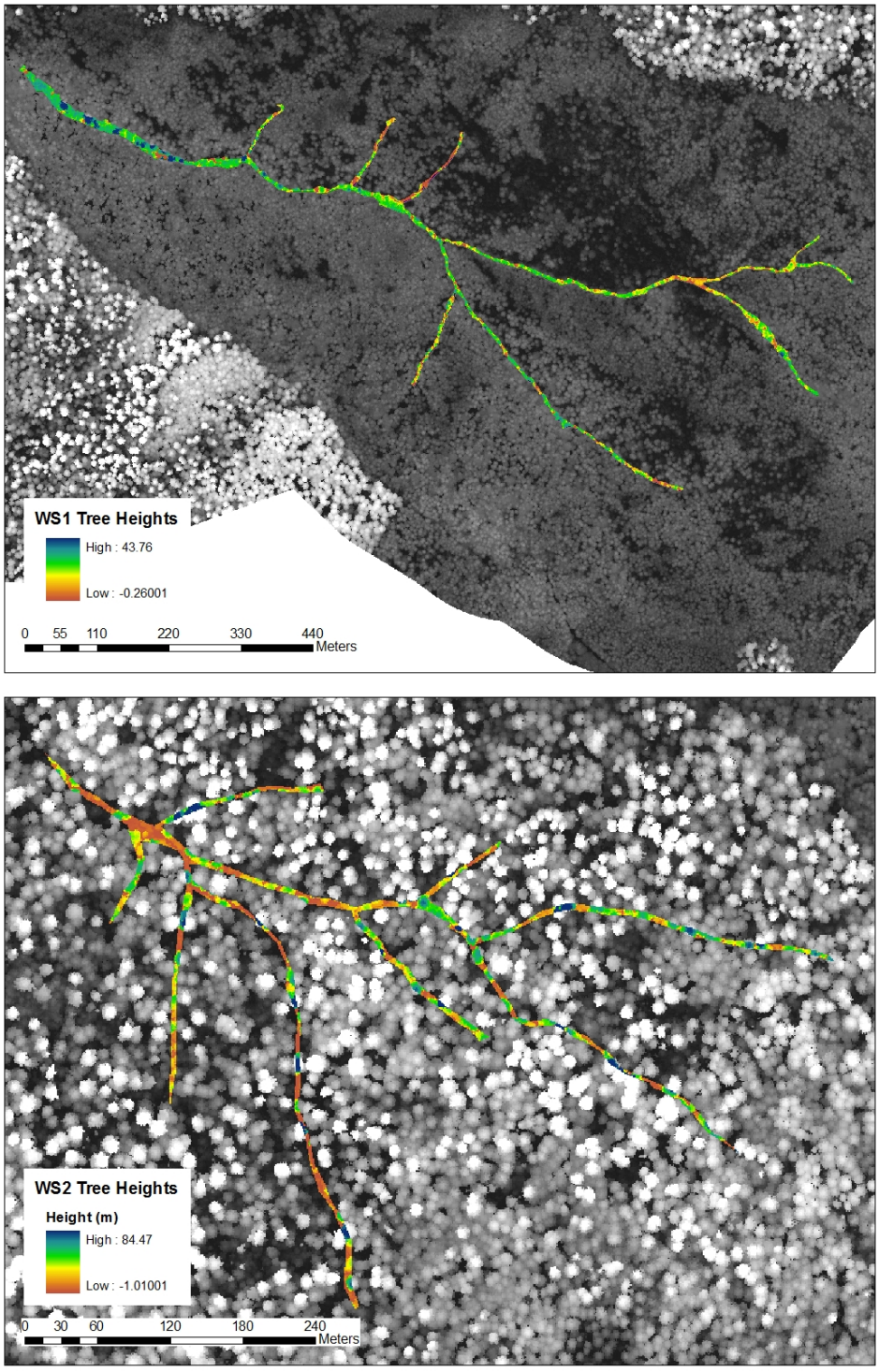

Figure 16: Tree height LiDAR data with channel areas colored for watersheds 1 and 2

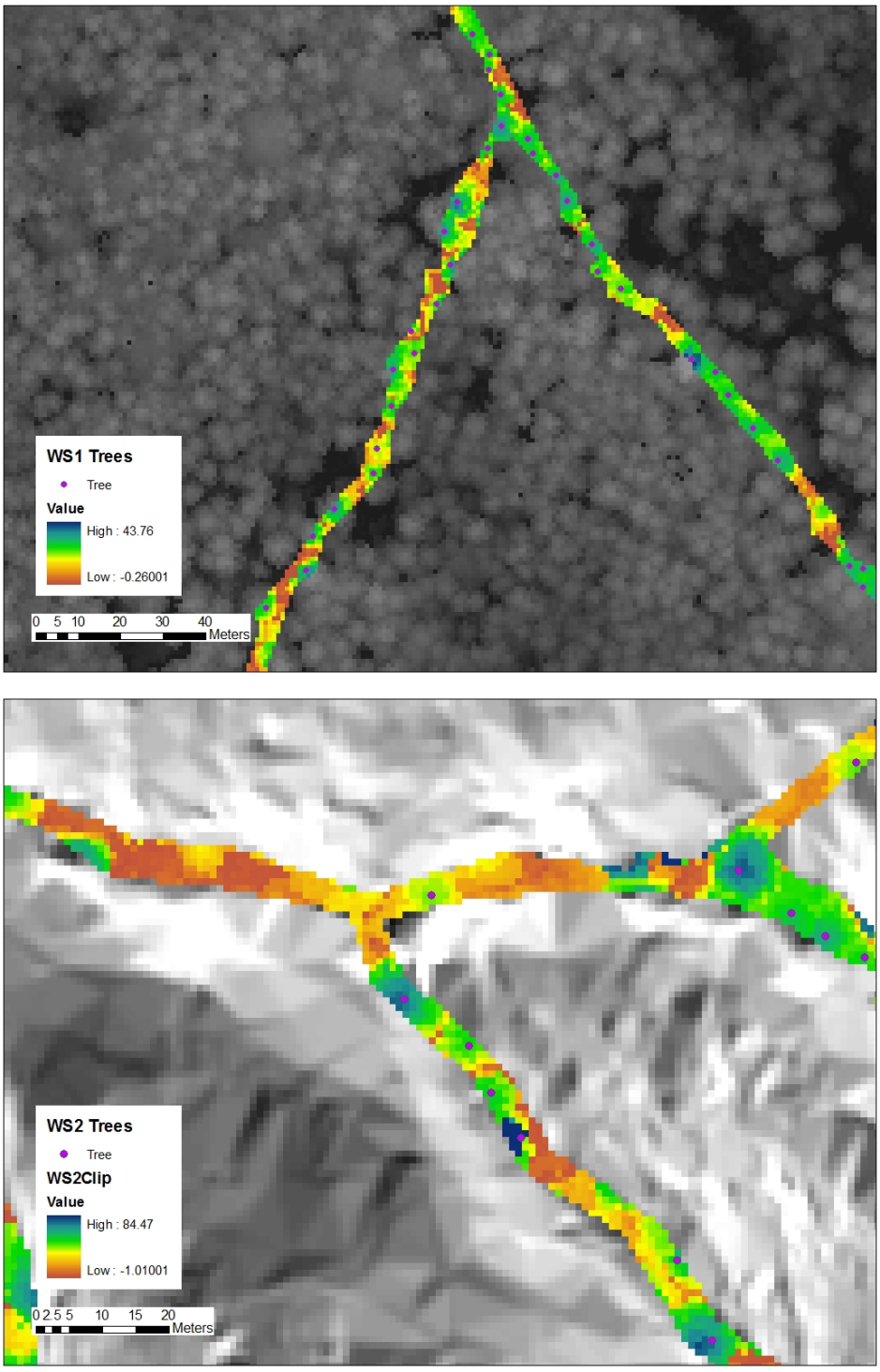

Figure 17: Examples of tree selection for watersheds 1 and 2

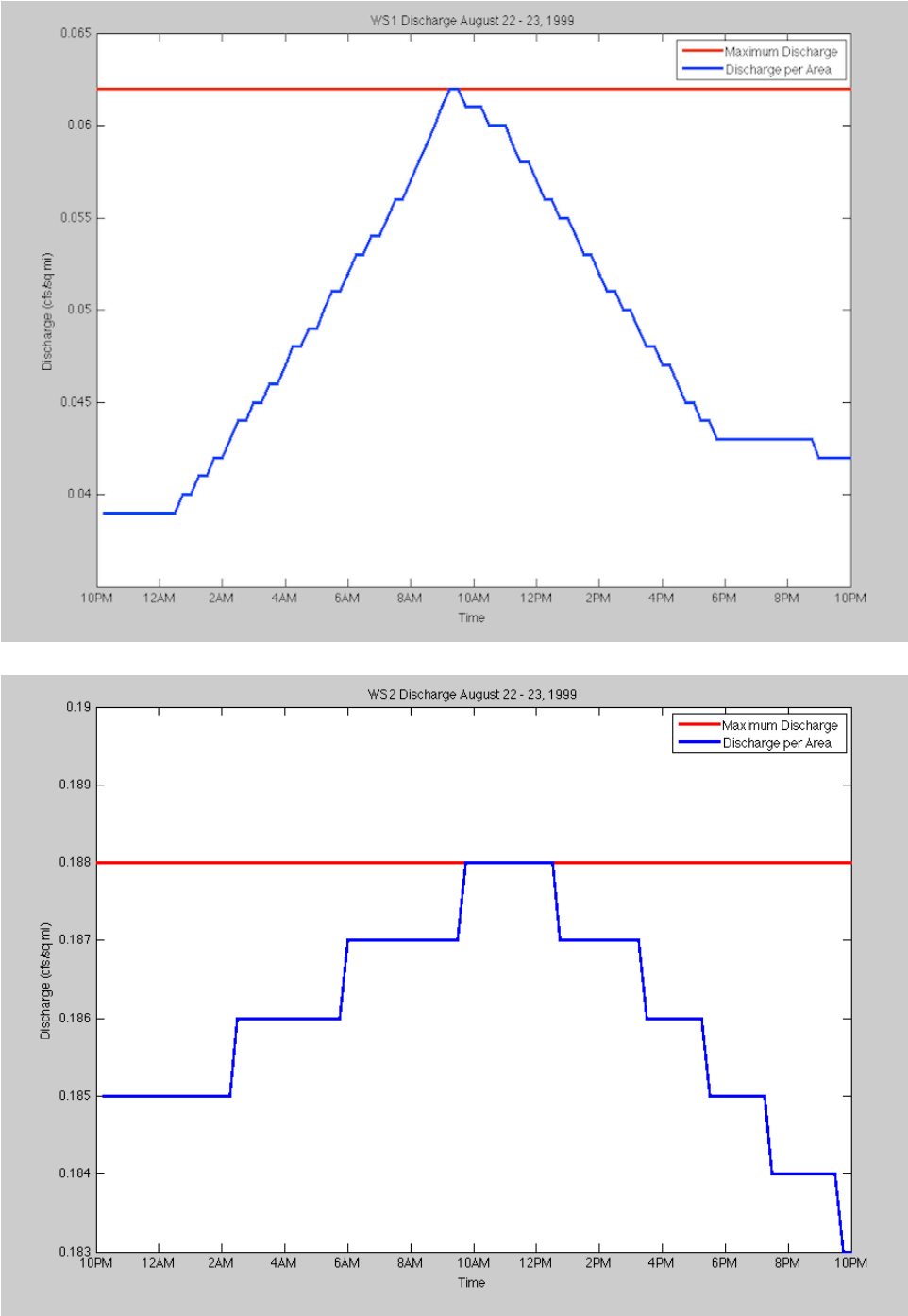

Figure 18: Stream gage data used to estimate water lost to ET for both watersheds 1 and 2

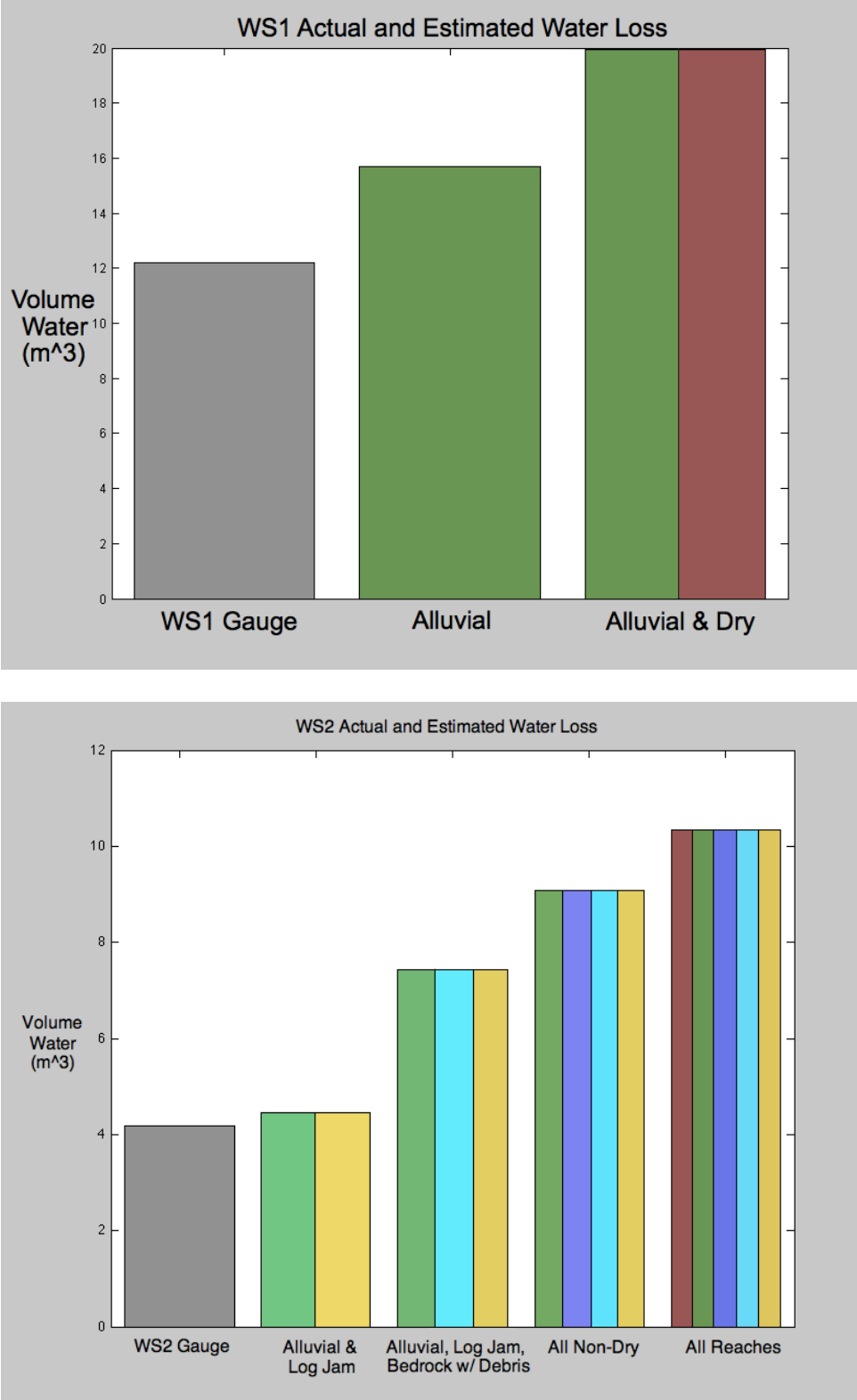

Figure 19: Comparison of estimated water loss at stream gage (*gray*) to estimated ET water loss for various combinations of trees by reach lithology (*colors represent reaches included as per legend for Figure 15)*

Table 1:

WS	Area	Min-max elevation	Channel length	Slope %	Management	Vegetation
1	95.9	457-1027	2808	59	100% clearcut 1962-66; prescribed burned 1967	Red Alder/Douglas fir
2	60.3	548-1078	1861	53	control	Douglas fir/Western hemlock
3	101.1	418-1080	2771	52	1.5 km roads, 1959; 25% clearcut in 3 patches, 1963	Douglas fir/Western hemlock
6	13	897-1029	112	25	100% clearcut 1974	Douglas fir
7	15.4	938-1102	125	34	50% selective canopy removal 1974; remaining canopy removed 1984	Douglas fir
8	21.4	993-1182	318	26	control	Western hemlock/Silver fir
9	8.5	432-731	NA	58	control	Douglas fir/Western hemlock
10	10.2	473-679	456	58	100% clearcut 1975	Douglas fir